MDS.[13–15] In fact, the prognostic value of these two chromosome aberration groups was not significantly different among AML patients,[15] but sufficient data for MDS were lacking. The present study demonstrates that the prognosis of patients who carry −5 and del(5q) are significantly different, as OS and LFS of −5 group were shorter than del(5q) patients even if 5q- syndrome patients were excluded from del(5q) patients (Figure 2 and data not shown). AML patients with monosomy 7 rather than with deleted 7q chromosome were reported to lead to poor prognosis.[16] Significantly poor prognosis of −5 group in our series might be explained by the observation that −5 was significantly correlated with presence of monosomy 7 as compared to del(5q) group ($P<0.001$). The co-presence of chromosomes 5 and 7 abnormalities has been associated with poor outcomes in MDS and AML.[17–22]

Although the cause of leukemic progression is unknown, susceptibility to leukemia clearly leads to higher mortality of −5 patients compared to del(5q) patients (Figure 2b). The −5 group also had significantly more severe neutropenia and thrombocytopenia and might exacerbate the survival of this group (Figures 1b and c). Neutropenia and thrombocytopenia, but not severe anemia, are reported to be common findings of patients with monosomy 7.[23] Taken together, laboratory findings shown in −5 group and high incidence of the co-presence of −5 and monosomy 7 might result in poor prognosis of the corresponding patients.

In this survey, the incidence of 5q- syndrome was quite rare in Japan. Recent studies suggest different genetic or environmental backgrounds between Asian and Western MDS populations.[24,25] According to the recent report by Haase *et al.*,[28] isolated del(5q) was seen in 14%, del(5q) with one additional abnormality in 5%, and complex abnormalities including del(5q) were seen in 11% of patients with clonal abnormalities. In the Korean study, isolated del(5q) was seen in 1.7% of the patients.[24] The incidence of del(5q), isolated del(5q) and 5q- syndrome patients was 8.4, 2.2 and 1.3%, respectively, in Japanese MDS study. These data are lower than those of Western patients but more similar to those of Asian patients.[24–26]

In the present study, we paid particular attention to MDS patients with del(5q) and classified them into four groups according to the cytogenetic complexity: 5q-, 7+, complex and other. 5q- patients have previously been well defined as having relatively good prognosis, whereas poor prognosis was indicated when it was combined with other anomalies.[19,20,26,27] OS and LFS of 7+ group were significantly shorter than 5q- group and OS of complex was significantly shorter than 5q-(Figure 3a and data not shown). It is suggested that the clinical outcome of MDS patients with del(5q) depends on the prognostic value of combined chromosomal abnormalities.

The most significant independent prognostic variables in MDS are the percentage of bone marrow blasts, the number of cytopenias and cytogenetic pattern. By weighting these variables according to their statistic power, IPSS separates MDS patients into four distinct risk groups regarding survival and the potential for leukemic progression: low risk, Int-1, Int-2 and high risk.[10] Even in the del(5q) patient group, which is considered to have a better prognosis, univariate analysis and multivariate analysis of del(5q) patients in our series showed that the cytogenetic pattern, percentage of bone marrow blasts and platelet transfusion dependency were the most relevant risk factors (Tables 2 and 3). Figures 3b and c show that IPSS critically determines OS and LFS of del(5q) patients. All 21 patients classified as 5q- syndrome were low risk of IPSS, and the patients classified as high risk were AML and refractory anemia with excess blasts (RAEB)-2 cases with adverse chromosomal abnormalities.

As for the del(5q) patients who are far from the risk of leukemic progression, red cell transfusion dependency often has an adverse impact on survival.[28] Although red cell transfusion dependency was not a significant prognostic factor by the present analyses, the degree of anemia had a tendency to affect survival of these patients from the result of univariate analysis ($P=0.059$, Table 2).

Although IPSS is based on FAB classification and does not take into account other prognostic factors such as dysplasia and transfusion requirement, WPSS has a relevant prognostic value.[29] Therefore, we applied WPSS to our patient data (Figure 3d) and confirmed that WPSS can predict the prognosis of del(5q) MDS patients more clearly than IPSS.

Our study demonstrated that −5 and del(5q) belong to different clinical entities and their biological behaviors are different from each other, and that del(5q) patients can be stratified according to their additional chromosomal abnormalities and IPSS or WPSS status. Severe anemia requires frequent transfusions, reduces quality of life and becomes often the major clinical problem for MDS patients with del(5q). The prognosis of del(5q) patients is related to their status of chromosomal abnormalities and transfusion dependency, but new agents such as lenalidomide improve the disorder and might provide new insights into more precise understanding of the disease.[30]

## Acknowledgements

We greatly thank the hospitals that provided patient data as described in the Supplementary Information, and also thank Ms Aki Tochigi for the paper preparation. This study was supported by the grant of the Japanese Cooperative Study Group for Intractable Bone Marrow Diseases, Ministry of Health, Labor and Welfare of Japan.

## References

1 Nimer SD, Golde DW. The 5q- abnormality. *Blood* 1987; **70**: 1705–1712.
2 Van den Berghe H, Michaux L. 5q-, twenty-five years later: a synopsis. *Cancer Genet Cytogenet* **94**: 1–7.
3 Giagounidis AA, Germing U, Haase S, Hildebrandt B, Schlegelberger B, Schoch C *et al.* Clinical, morphological, cytogenetic, and prognostic features of patients with myelodysplastic syndromes and del(5q) including band q31. *Leukemia* 2004; **18**: 113–119.
4 Giagounidis AA, Germing U, Wainscoat JS, Boultwood J, Aul C. The 5q- syndrome. *Hematology* 2004; **9**: 271–277.
5 Van den Berghe H, Cassiman JJ, David G, Fryns JP, Michaux JL, Sokal G. Distinct haematological disorder with deletion of long arm of no. 5 chromosome. *Nature* 1974; **251**: 437–438.
6 Giagounidis AA, Germing U, Strupp C, Hildebrandt B, Heinsch M, Aul C. Prognosis of patients with del(5q) MDS and complex karyotype and the possible role of lenalidomide in this patient subgroup. *Ann Hematol* 2005; **84**: 569–571.
7 Malcovati L, Porta MG, Pascutto C, Invernizzi R, Boni M, Travaglino E *et al.* Prognostic factors and life expectancy in myelodysplastic syndromes classified according to WHO criteria: a basis for clinical decision making. *J Clin Oncol* 2005; **23**: 7594–7603.
8 Van den Berghe H, Vermaelen K, Mecucci C, Barbieri D, Tricot G. The 5q- anomaly. *Cancer Genet Cytogenet* 1985; **17**: 189–255.
9 Greenberg P, Cox C, LeBeau MM, Fenaux P, Morel P, Sanz G *et al.* International scoring system for evaluating prognosis in myelodysplastic syndromes. *Blood* 1997; **89**: 2079–2088.
10 Harris NL, Jaffe ES, Diebold J, Flandrin G, Muller-Hermelink HK, Vardiman J *et al.* World Health Organization classification of neoplastic diseases of the hematopoietic and lymphoid tissues:

report of the Clinical Advisory Committee meeting-Airlie House, Virginia, November 1997. *J Clin Oncol* 1999; **17**: 3835–3849.
11 Malcovati L, Germing U, Kuendgen A, Porta D, Pascutto C, Invernizzi R *et al.* Time-dependent prognostic scoring system for predicting survival and leukemic evolution in myelodysplastic syndromes. *J Clin Oncol* 2007; **25**: 3503–3510.
12 Bennett JM, Catovsky D, Daniel MT, Flandrin G, Galton DA, Gralnick HR *et al.* Proposals for the classification of the myelodysplastic syndromes. *Br J Haematol* 1982; **51**: 189–199.
13 Dastugue N, Payen C, Lafage-Pochitaloff M, Bernard P, Leroux D, Huguet-Rigal F *et al.* Prognostic significance of karyotype in *de novo* adult acute myeloid leukemia. The BGMT group. *Leukemia* 1995; **9**: 1491–1498.
14 Mauritzson N, Johansson B, Albin M, Rylander L, Billstrom R, Ahlgren T *et al.* Survival time in a population-based consecutive series of adult acute myeloid leukemia the prognostic impact of karyotype during the time period 1976–1993. *Leukemia* 2000; **14**: 1039–1043.
15 Grimwade D, Walker H, Oliver F, Wheatley K, Harrison C, Harrison G *et al.* The importance of diagnostic cytogenetics on outcome in AML: analysis of 1612 patients entered into the MRC AML 10 trial. The Medical Research Council Adult and Children's Leukaemia Working Parties. *Blood* 1998; **92**: 2322–2333.
16 Hasle H, Alonzo TA, Auvrignon A, Behar C, Chang M, Creutzig U *et al.* Monosomy 7 and deletion 7q in children and adolescents with acute myeloid leukemia: an international retrospective study. *Blood* 2007; **109**: 4641–4647.
17 Morel P, Hebbar M, Lai JL, Duhamel A, Preudhomme C, Wattel E *et al.* Cytogenetic analysis has strong independent prognostic value in *de novo* myelodysplastic syndromes and can be incorporated in a new scoring system: a report on 408 cases. *Leukemia* 1993; **7**: 1315–1323.
18 Toyama K, Ohyashiki K, Yoshida Y, Abe T, Asano S, Hirai H *et al.* Clinical implications of chromosomal abnormalities in 401 patients with myelodysplastic syndromes: a multicentric study in Japan. *Leukemia* 1993; **7**: 499–508.
19 Jacobs RA, Combleet M, Vardiman J, Larson R, LeBeau MM, Rowley JD. Prognostic implications of morphology and karyotype in primary myelodysplastic syndromes. *Blood* 1986; **67**: 1765–1772.
20 Yunis JJ, Lobell M, Arnesen MA, Oken MM, Mayer MG, Rydell RE *et al.* Refined chromosome study helps define prognostic subgroups in most patients with primary myelodysplastic syndrome and acute myelogenous leukaemia. *Br J Haematol* 1988; **68**: 189–194.
21 Pierre R, Catovsky D, Mufti G, Swansbury G, Mecucci C, Dewald GW *et al.* Clinical cytogenetic correlations in myelodysplasia (preleukemia). *Cancer Genet Cytogenet* 1989; **40**: 149–161.
22 Samuels BL, Larson RL, LeBeau MM, Daly KM, Bitter MA, Vardiman JW *et al.* Specific chromosomal abnormalities in acute nonlymphocytic leukemia correlate with drug susceptibility *in vivo*. *Leukemia* 1988; **2**: 79–83.
23 Kardos G, Baumann I, Passmore SJ, Locatelli F, Hasle H, Schultz KR *et al.* Refractory anemia in childhood: a retrospective analysis of 67 patients with particular reference to monosomy 7. *Blood* 2003; **102**: 1997–2003.
24 Lee JH, Lee JH, Shin YR, Lee JS, Kim WK, Chi HS *et al.* Application of different prognostic scoring systems and comparison of the FAB and WHO classifications in Korean patients with myelodysplastic syndrome. *Leukemia* 2003; **17**: 305–313.
25 Chen B, Zhao WL, Jin J, Xue YQ, Cheng X, Chen XT *et al.* Clinical and cytogenetic features of 508 Chinese patients with myelodysplastic syndrome and comparison with those in Western countries. *Leukemia* 2005; **19**: 767–775.
26 Sokal G, Michaux JL, van den Berghe H, Cordier A, Rodhain J, Ferrantr A *et al.* A new hematologic syndrome with a distinct karyotype: the 5q- chromosome. *Blood* 1975; **46**: 519–533.
27 Dewald GW, Davis MP, Pierre RV, O'Fallon JR, Hoagland HC. Clinical characteristics and prognosis of 50 patients with a myeloproliferative syndrome and deletion of part of the long arm of chromosome 5. *Blood* 1985; **66**: 189–197.
28 Haase D, Germing U, Schanz J, Pfeilstöcker M, Nösslinger T, Hildebrandt B *et al.* New insights into the prognostic impact of the karyotype in MDS and correlation with subtypes: evidence from a core dataset of 2124 patients. *Blood* 2007; **110**: 4385–4395.
29 Malcovati L, Porta MG, Pascutto C, Invernizzi R, Boni M, Travaglino E *et al.* Prognostic factors and life expectancy in myelodysplastic syndromes classified according to WHO criteria: a basis for clinical decision making. *J Clin Oncol* 2005; **23**: 7594–7603.
30 List AF, Baker AF, Green S, Bellamy W. Lenalidomide: targeted anemia therapy for myelodysplastic syndromes. *Cancer Control* 2006; **13**: 4–11.

Supplementary Information accompanies the paper on the Leukemia website (http://www.nature.com/leu)

# Kpm/Lats2 is linked to chemosensitivity of leukemic cells through the stabilization of p73

Masahiro Kawahara,[1] Toshiyuki Hori,[1] Kazuhisa Chonabayashi,[1] Tsutomu Oka,[2] Marius Sudol,[2,3] and Takashi Uchiyama[1]

[1]Department of Hematology and Oncology, Graduate School of Medicine, Kyoto University, Kyoto, Japan; [2]Laboratory of Signal Transduction and Proteomic Profiling, Weis Center for Research, Danville, PA; and [3]Department of Medicine, Mount Sinai School of Medicine, New York, NY

**Down-regulation of the Kpm/Lats2 tumor suppressor is observed in various malignancies and associated with poor prognosis in acute lymphoblastic leukemia. We documented that Kpm/Lats2 was markedly decreased in several leukemias that were highly resistant to conventional chemotherapy. Silencing of Kpm/Lats2 expression in leukemic cells did not change the rate of cell growth but rendered the cells more resistant to DNA damage–inducing agents. Expression of p21 and PUMA was strongly induced by these agents in control cells, despite defective p53, but was only slightly induced in Kpm/Lats2-knockdown cells. DNA damage–induced nuclear accumulation of p73 was clearly observed in control cells but hardly detected in Kpm/Lats2-knockdown cells. Chromatin immunoprecipitation (ChIP) assay showed that p73 was recruited to the *PUMA* gene promoter in control cells but not in Kpm/Lats2-knockdown cells after DNA damage. The analyses with transient coexpression of Kpm/Lats2, YAP2, and p73 showed that Kpm/Lats2 contributed the stability of YAP2 and p73, which was dependent on the kinase function of Kpm/Lats2 and YAP2 phosphorylation at serine 127. Our results suggest that Kpm/Lats2 is involved in the fate of p73 through the phosphorylation of YAP2 by Kpm/Lats2 and the induction of p73 target genes that underlie chemosensitivity of leukemic cells. (Blood. 2008;112:3856-3866)**

## Introduction

The *Warts* (*Wts*) tumor suppressor gene (also termed *Lats* after large tumor suppressor) was first identified by mitotic recombination of somatic cells and screening for homozygous mutants with overproliferation phenotype in *Drosophila melanogaster*.[1,2] This discovery initiated a series of genetic studies in *Drosophila* that led to the delineation of a new signaling network named the Hippo pathway, which is now known to regulate cell growth, cell survival, and organ size in developing animals.[3-5] This pathway consists of a kinase cascade in its core where Hippo (Hpo) phosphorylates and activates Wts/Lats,[6] which then in turn phosphorylates and inactivates Yorkie (Yki), a transcription coactivator. Inactivation of Yki results in control of cell survival and cell growth through down-regulation of *Drosophila* inhibitor of apoptosis 1 (Diap1) and Cyclin E.[7] Salvador (Sav),[8,9] a scaffold protein for Hpo, and Mats (mob as tumor suppressor),[10-12] a partner and potentiater of Wts, are also essential components of this pathway. Furthermore, recent evidence has placed Expanded (EX), Merlin (Mer),[13] both 4.1 family proteins, and Fat (FT),[14-17] the atypical cadherin, in the upstream of the Hippo pathway although their connection to the kinase cascade is largely based on genetic epitasis. The Hippo pathway is believed to be conserved throughout species because some of the mammalian homologues have been shown to compensate the corresponding defects in the *Drosophila* Hippo pathway. At present, however, only a small part of the mammalian Hippo pathway has been experimentally substantiated.

*Kpm* (alternatively named Lats2) is one of the 2 human homologues of *Drosophila Wts*.[18,19] In parallel to *Drosophila Wts*, we and others have shown the critical involvement of *Kpm*/Lats2 in regulation of cell growth and survival. Kpm/Lats2 overexpression results in the cell cycle arrest in G2/M phase via inhibition of Cdc2–Cyclin B kinase activity leading eventually to apoptosis,[20] inhibition of G1/S transition via down-regulation of Cyclin E/Cdk2 kinase activity,[21] or apoptosis via down-regulation of Bcl-2 and Bcl-xL.[22] Kpm/Lats2 binds to Mdm2 and inhibits its E3 ubiquitin ligase activity, resulting in the stabilization of p53 and leading to the p53-dependent G1/S arrest in nocodazole-treated cells.[23] Moreover, Kpm/Lats2 is a target gene of p53 both in mammalian as well as in *Drosophila* cells,[24,25] suggesting that Kpm/Lats2 may be a positive-feedback-loop regulator of p53. Kpm/Lats2 knockout mice are embryonically lethal and fibroblasts isolated from these mice appear to be defective in contact inhibition and display genomic instability through multipolar mitotic spindles.[26,27] Mst-2, one of the mammalian orthologues of *Drosophila* Hippo, has been reported to phosphorylate Kpm/Lats2 as well as its related kinase, Lats1.[28] However, the downstream function of Kpm/Lats2 has not been elucidated in the Hippo pathway in mammals, because the interaction between Kpm/Lats2 and Yes-associated protein (YAP), the mammalian orthologue of Yki, has not been shown.

Yes-kinase associated protein (YAP) was initially isolated by virtue of its binding to the Src family member, a nonreceptor tyrosine kinase Yes.[29,30] The cloning of YAP revealed a new modular protein domain, known today as the WW domain, which recognizes a specific set of proline-rich ligands. The YAP gene encodes at least 2 isoforms: YAP1 and YAP2, which are generated by differential splicing and differ in the number of WW domains they contain. YAP1 has one WW domain and YAP2 has 2 WW domains.[30,31] In human epithelial cells, YAP plays a potentially oncogenic role through several signaling interactions with potent

Submitted September 12, 2007; accepted April 19, 2008. Prepublished online as *Blood* First Edition paper, June 18, 2008; DOI 10.1182/blood-2007-09-111773.

The online version of this article contains a data supplement.

The publication costs of this article were defrayed in part by page charge payment. Therefore, and solely to indicate this fact, this article is hereby marked "advertisement" in accordance with 18 USC section 1734.

signaling proteins.[32-36] Furthermore, a region of human chromosome 11 at position q22 has been reported to be frequently amplified in various cancers, and this amplicon contains *YAP* and *cIAP2* loci.[37,38] Curiously, YAP has also been shown to regulate apoptosis. For example, YAP forms a signaling complex with p53-binding protein-2, a known regulator of the apoptotic activity of p53.[39,40] YAP interacts with and coactivates p73 to induce transcription of its target genes, leading to apoptosis and cell cycle arrest.[41] In sum, YAP has a capacity to function either as an oncogene or as a proapoptotic factor.

Recent clinical studies have indicated that the expression level of Kpm/Lats2 correlates with clinical course of some malignancies. Down-regulation of Kpm/Lats2 was associated with larger tumor size and high number of metastatic lymph nodes in breast cancers,[42] and it was significantly associated with poor prognosis in acute lymphoblastic leukemia (ALL).[43] The relative level of Kpm/Lats2 expression was shown with high confidence as the most important prognostic factor in predicting disease-free survival in ALL, even compared with the *BCR-ABL* gene fusion, which is so far the most significant factor for poor prognosis. However, the molecular and cellular mechanisms underlying the poor clinical course in leukemias that have a relatively low level of Kpm/Lats2 expression have not been investigated in detail.

In the present study, we documented that Kpm/Lats2 was down-regulated also in adult T-cell leukemia (ATL) and natural killer (NK) leukemia/lymphoma, both of which are known to be highly resistant to conventional chemotherapy. Then we addressed the molecular mechanism underlying the chemoresistance associated with low Kpm/Lats2 expression. We herewith report that down-regulation of Kpm/Lats2 leads to chemoresistance through insufficient nuclear accumulation of p73, resulting in poor induction of its target genes p21 and p53 up-regulated modulator of apoptosis (PUMA).

## Methods

### Cells and cell culture

Leukemic cell lines including KG-1a[44] were cultured in 10% heat-inactivated fetal bovine serum (FBS; Invitrogen, Paisley, United Kingdom) containing Iscove modified Dulbecco medium (IMDM; Invitrogen) with 2 mM L-glutamine and antibiotics (Invitrogen), and only ED-40515$^{+}$[45] was cultured in the same medium with 100 IU/mL recombinant human interleukin-2 (rhIL-2; Shionogi, Osaka, Japan). Adherent cell lines including 293T, GP2-293, and HeLa were cultured using Dulbecco modified Eagle medium (DMEM; Invitrogen) instead of IMDM. All cells were maintained at 37°C in a 5% $CO_2$ humidified incubator. Clinical samples from patients with leukemia were cryopreserved in our laboratory as described previously.[46-48] Normal peripheral mononuclear cells (PBMCs) were purified from healthy donor with informed consent; normal CD4$^{+}$ T cells and normal CD56$^{+}$ cells were purified using magnetic-activated cell sorting (MACS) CD4$^{+}$ T-cell isolation kit (Miltenyi Biotec, Bergisch Gladbach, Germany) and MACS CD56$^{+}$ isolation kit (Miltenyi Biotec), respectively. All the clinical samples were taken with informed consent and used only for in vitro study following the guideline of the institutional review board of Kyoto University. This study was conducted in accordance with the Declaration of Helsinki.

### Isolation of total RNA and quantitative real-time PCR

The isolation of total RNA was performed using RNeasy Mini kit (Qiagen, Valencia, CA). The cDNA was synthesized from 1 μg total RNA by ImProm-II Reverse Transcription system (Promega, Madison, WI). Quantitative real-time polymerase chain reaction (PCR) was analyzed using SYBR Green (Invitrogen) on an ABI Prism 7900HT instrument (Applied Biosystems, Foster City, CA). More than one internal control was always used in each analysis, and only when relative amounts of internal controls were constant for each sample, were data considered valid. The list of gene-specific primers is provided in Table 1.

**Table 1. Primer sequence for real-time PCR or semiquantitative RT-PCR**

| Gene | Primer sequence |
|---|---|
| **Kpm (for RT-PCR)** | |
| Forward | GCTGACTTTGGCCATTGAGAGTGTC |
| Reverse | CATCTACGGGGTCGAAATTCGAGGT |
| **Kpm (for real-time)** | |
| Forward | GTTCAGGTGGACTCACAATTCC |
| Reverse | CGACAGTTAGACACATCATCCCA |
| **Lats1** | |
| Forward | TGGTCATATTAAATTGACTGAC |
| Reverse | CCACATCGACAGCTTGAGGG |
| **YAP** | |
| Forward | TGGGAGATGGCAAAGACATCTTCTG |
| Reverse | ACACTGGATTTTGAGTCCCACCATC |
| **cIAP1** | |
| Forward | CAGCCTGAGCAGCTTGCAA |
| Reverse | CAAGCCACCATCACAACAAAA |
| **cIAP2** | |
| Forward | TCCGTCAAGTTCAAGCCAGTT |
| Reverse | TCTCCTGGGCTGTCTGATGTG |
| **survivin** | |
| Forward | TGCCTGGCAGCCCTTTC |
| Reverse | CCTCCAAGAAGGGCCAGTTC |
| **XIAP** | |
| Forward | AGTGGTAGTCCTGTTTCAGCATCA |
| Reverse | CCGCACGGTATCTCCTTCA |
| **bcl-2** | |
| Forward | AGGAAGTGAACATTTCGGTGAC |
| Reverse | GCTCAGTTCCAGGACCAGG |
| **p21** | |
| Forward | CTGTCACTGTCTTGTACCCT |
| Reverse | GGTAGAAATCTGTCATGCTGC |
| **PUMA** | |
| Forward | GACCTCAACGCACAGTA |
| Reverse | CTAATTGGGCTCCATCT |
| **TAp73** | |
| Forward | GCACCACGTTTAAGCACCTCT |
| Reverse | GCAGATTGAACTGGGCCATGA |
| **β-actin** | |
| Forward | TCCTGTGGCATCCACGAAACT |
| Reverse | GAAGCATTTGCGGTGGACGAT |
| **hprt** | |
| Forward | TGACACTGGCAAAACAATGCA |
| Reverse | GGTCCTTTTCACCAGCAAGCT |
| **gapdh** | |
| Forward | GAAGGTGAAGGTCGGAGTC |
| Reverse | GAAGATGGTGATGGGATTTC |

### Plasmids

The plasmids for expression of HA-tagged Kpm wild-type (wt) form and Kpm-kinase dead (kd) form (mutant form K697 to A) were described before.[18] FLAG-tagged YAP1, YAP1-S127A (mutant form S127 to A; S127 is Akt-phosphorylation site), YAP1-WW* (mutant form of WW domain), YAP2, YAP2-S127A, YAP2-1WW* (mutant form of first WW domain), and YAP2-2WW* (mutant form of second WW domain) inserted into pFLAG-CMV2 vector were described previously 33. TAp73α inserted into pcDNA3 vector, described elsewhere,[49] was a gift of Dr Yoshihide Ueda (Kyoto University). The plasmid expressing Kpm/Lats2 shRNA was generated by insertion of target sequence (loop sequence, CTGTGAAGC-CACAGATGGG) and target antisense sequence into the retrovirus (RV)

vector, pSINsi-hU6 (Takara, Kusatsu, Japan). Kpm/Lats2 target sequence is TTCACCTTCCGAAGGTTCT; control sequence is TCGTACTCTCGTCTTCGAT. Control sequence was constructed by shuffling Kpm/Lats2 target sequence, and it was confirmed using BLASTN that control sequence did not target any other genes.[50] p73 target sequence is GGATTCCAGCATGGACGTCTT, as described elsewhere.[51] pVSV-G was used as the envelope plasmid.

### Plasmid transfection and retrovirus vector transduction

Plasmids were transfected into 293T cells using CalPhos mammalian transfection kit (Clontech, Mountain View, CA) or FuGENE-HD (Roche, Basel, Switzerland) for coimmunoprecipitation assays. Retroviruses were generated by cotransfection of shRNA containing retrovirus vector and pVSV-G into GP2-293 packaging cells with CalPhos kit and collected by ultracentrifugation. Retronectin (Takara) was used to transduce leukemic cells with retroviruses. After transduction, pools of cells in bulk selected with 0.5 mg/mL G-418 (Nacalai Tesque, Kyoto, Japan) were used in the following assays.

### MTT assay

To evaluate cell viability, an appropriate number of cells were seeded with doxorubicin (DXR; Pharmacia, Milan, Italy) or etoposide (ETP; Bristol-Myers, New York, NY) in appropriate concentrations. Next MTT assays were performed using WST-8 (Nacalai Tesque) according to the manufacturer's protocol and analyzed with microplate reader Benchmark (Bio-Rad, Hercules, CA) as described previously.[20]

### Antibodies, immunoprecipitation, and Western blotting

The following antibodies were purchased or prepared in our laboratory: anti-FLAG mouse monoclonal antibody (Sigma-Aldrich, St Louis, MO), anti-HA mouse monoclonal antibody (Roche), anti-YAP rabbit polyclonal antibody, anti–phospho-YAP(Ser127) rabbit polyclonal antibody, anti-PUMA rabbit polyclonal antibody, anti-p21 mouse monoclonal antibody (Cell Signaling, Beverly, MA), anti-p73 mouse monoclonal antibody (Ab-4; Lab Vision, Fremont, CA), antiactin goat polyclonal antibody (Santa Cruz Biotechnology, Santa Cruz, CA), HRP conjugated anti–mouse IgG and anti–rabbit IgG (GE Healthcare, Uppsala, Sweden), and anti–goat IgG (Santa Cruz Biotechnology). Anti-Kpm rabbit polyclonal antibody was generated in our laboratory as described previously.[18] For immunoprecipitation assay, cells were lysed on ice for 30 minutes with Triton X–based lysis buffer (50 mM Tris-HCl at pH 8.0, 150 mM NaCl, 1% Triton X, 1 mM PMSF, 1 mM EDTA, and protease inhibitor cocktail; Nacalai Tesque), with the optional addition of phosphatase inhibitor cocktail 1 and 2 (Sigma-Aldrich) to detect phosphorylation status of YAP. The lysate, after centrifugation and precleaning, was incubated with 1 μg indicated antibodies overnight at 4°C and precipitated with protein G–sepharose beads (GE Healthcare) at 4°C for 3 hours. After washing 5 times with lysis buffer, the precipitate was boiled in 2 × sample buffer. Phosphatase treatment of the immunoprecipitates was done by incubating beads with 0.2 U/μL calf intestine phosphatase (CIP; Sigma-Aldrich) in 10 μL of 100 mM Tris-HCl (pH 8.0) at 37°C for 1 hour. Western blotting was performed according to the manufacturer's protocol for each antibody, and the protein bands were detected using the enhanced chemiluminescence (ECL) detection system (GE Healthcare).

### Immunofluorescence microscopy

KG-1a cells were treated with 0.1 μg/mL ETP for 2.5 days. Then cells were cytospun on glass slides and fixed in ice-cold acetone for 3 minutes. After blocking, cells were incubated with 4 μg/mL anti-p73 mouse monoclonal antibody (Lab Vision) or mouse control IgG (Santa Cruz Biotechnology) in 1% bovine serum albumin containing PBS for 1 hour at room temperature. After extensive wash, cells were incubated with Alexa Fluor-488–conjugated anti–mouse IgG (Invitrogen), and 4′,6-diamino-2-phenylindole (DAPI; Sigma-Aldrich) staining was finally performed. Analysis was performed with fluorescence microscopy BIOZERO B8-8100 (Keyence, Osaka, Japan) that was equipped with a camera as an all-in-one type and with objective lenses (4×/0.2 NA and 20×/0.75 NA). B2-Viewer versus 1.0 (Keyence) and B2-Analyzer BZ-HIA versus 3.5 (Keyence) were used for image acquisition and image processing, respectively.

### Chromatin immunoprecipitation assay

Chromatin immunoprecipitation (ChIP) assay of p73 binding to sites in the PUMA promoter region was done using ChIP-IT enzymatic kits (Active Motif, Carlsbad, CA) according to the manufacturer's instructions. Briefly, cells were fixed with 1% formaldehyde for 10 minutes, lysed at 4°C for 30 minutes, homogenized by passing through 27-gauge needles, and centrifuged. Pelleted nuclei were then subjected to enzymatic sharing for the optimized time. One-tenth volume was stored as the input and the remaining was diluted and incubated with 2 μg anti-p73 antibody (Ab-4; Lab Vision) or control IgG (Santa Cruz Biotechnology) at 4°C overnight. Immune complexes were precipitated with protein G–sepharose beads. After intensive washes, beads were treated with elution buffer. The supernatants and the stored input solutions were reverse cross-linked and treated with RNase and proteinase K, and chromatin DNA was purified using the kit-included DNA minicolumns. The following PCR primers were used to amplify the *PUMA* gene promoter: 5′-tgactgggacccacagatcca-3′ (forward) and 5′-tccaggggaccctgttagtgag-3′ (reverse).

## Results

### Kpm/Lats2 is down-regulated in various leukemias

The down-regulation of Kpm/Lats2 has been linked to poor prognosis of ALL. To evaluate the significance of Kpm/Lats2 expression in other types of leukemia, we measured the expression level of Kpm/Lats2 by real-time PCR in leukemic cells that were available in our laboratory. The expression of Kpm/Lats2 was markedly decreased in all adult T-cell leukemia (ATL)–derived cell lines and all clinical samples from ATL patients in comparison with the normal counterpart $CD4^+$ T cells (Figure 1A). Similarly, down-regulation of Kpm/Lats2 was observed in one NK cell line and most of the clinical samples from patients with NK cell leukemia/lymphoma, compared with the normal counterpart $CD3^-$ $CD56^+$ NK cells (Figure 1B). Both types of leukemias are known to be clinically aggressive and resistant to conventional chemotherapy. In other leukemic cell lines derived from acute myeloid leukemia (AML) except for KG-1a, B-ALL (Burkitt leukemia), T-ALL, and T-chronic lymphocytic leukemia (T-CLL), the expression level of Kpm/Lats2 was very low or hardly detectable, compared with normal peripheral blood mononuclear cells (PBMCs; Figure S1, available on the *Blood* website; see the Supplemental Materials link at the top of the online article). These results suggest that the down-regulation of Kpm/Lats2 is rather common in hematologic malignancies and the degree of decrease may be associated with poor prognosis.

### Down-regulation of Kpm/Lats2 by shRNA does not affect the growth rate in 2 different leukemic cell lines

To delineate the cellular changes caused by Kpm/Lats2 down-regulation in leukemic cells, we made pools of Kpm/Lats2-knockdown KG-1a cells, a myeloid cell line, and ED-40515$^+$ cells, an ATL-derived cell line, using Kpm/Lats2-specific shRNA expression retrovirus vector. The reason why we chose these cell lines was because KG-1a and ED-40515$^+$ expressed relatively high levels of Kpm/Lats2 among myeloid and lymphoid cell lines, respectively (Figure 1A; Figure S1). Real-time PCR analyses of Kpm/Lats2 mRNA revealed that the expression levels of Kpm/Lats2 in Kpm/Lats2-knockdown KG-1a cells and ED-40515$^+$ cells was approximately 20% and approximately 30% of basal levels,

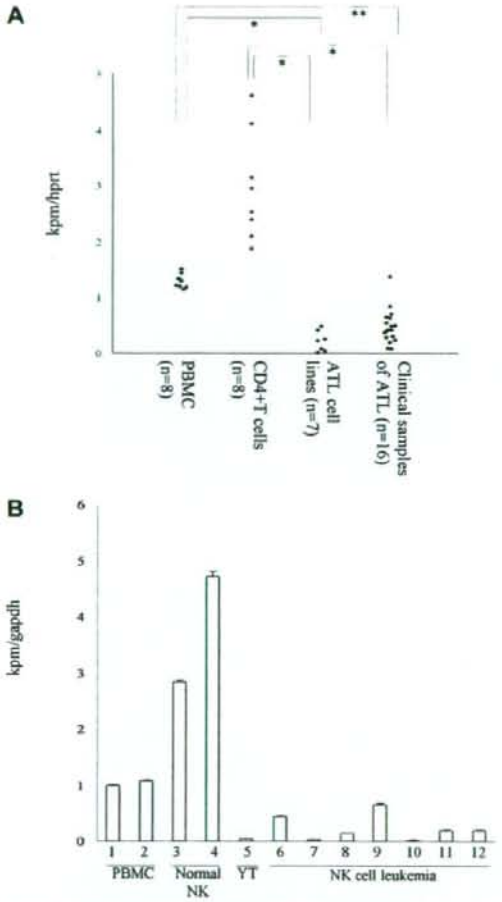


**Figure 1. Quantitative analysis of Kpm/Lats2 mRNA in clinical samples and cell lines.** (A) The amount of Kpm/Lats2 mRNA was measured in ATL cell lines, ATL clinical samples, normal PBMCs, and normal CD4$^+$ T cells. Data normalized to hprt are shown representatively in scale that the value for normal PBMC is 1. Normalization to gapdh gave similar results. The highest one among the ATL cell lines represents ED-40515$^+$. Analyses were performed in duplicate independently 3 times and representative data are shown (Welch $t$ test: $^*P < .001$; $^{**}P < .005$). (B) The amount of Kpm/Lats2 mRNA was measured in NK cell line (YT), NK cell leukemia clinical samples, normal PBMCs (lanes 1-2), and normal CD3$^-$56$^+$ NK cells (lanes 3-4), NK cell line (YT; lane 5), and NK cell leukemia clinical samples (lane 6-12). Data normalized to gapdh are shown as mean plus or minus SD in scale that the value for normal PBMCs (lane 1) is 1. Normalization to hprt gave similar results. Analyses were performed in triplicate independently twice, and representative data are shown.

respectively. There was no difference in the expression level of Lats1, the other human homologue of *Drosophila* Wts/Lats, between Kpm/Lats2-knockdown cells and wild-type or control cells (Figure 2A). We confirmed that Kpm/Lats2 expression was decreased also at the protein level in Kpm/Lats2-knockdown cells with Western blotting (Figure 2B).

Next we analyzed the growth rates of wild-type, Kpm/Lats2-knockdown, and control KG-1a cells as well as ED-40515$^+$ cells to determine whether the expression level of Kpm/Lats2 affected the duration of cell cycle. It has recently been reported that cell number of mouse embryonic fibroblasts (MEFs) from Kpm/Lats2 knockout mouse (Kpm/Lats2$^{-/-}$) was approximately 1.25-fold more than those from wild-type mouse (Kpm/Lats2$^{+/+}$) at day 4.[27] Contrary to this, there was no difference between growth rate of Kpm/Lats2-knockdown cells and that of wild-type or control cells during 96 hours as measured by MTT assay (Figure 2C) and cell counting assay with trypan blue dye exclusion (data not shown).

### Down-regulation of Kpm/Lats2 by shRNA in 2 different leukemic cell lines renders them resistant to DNA damage–inducing agents

To address whether down-regulation of Kpm/Lats2 renders leukemic cells resistant to DNA damage–inducing agents, we measured the cell viability of wild-type, Kpm/Lats2-knockdown, and control cells by MTT assay after the treatment with anticancer drugs, doxorubicin (DXR) or etoposide (ETP), which are used in standard chemotherapy for leukemia. The viability of these cells decreased after treatment of DXR or ETP in a dose-dependent and time-dependent manner but that of Kpm/Lats2-knockdown KG-1a cells was approximately 20% to 30% higher than that of wild-type or control KG-1a cells (Figure 2D). This tendency was also observed in ED-40515$^+$ cells, although the proportion of dead cells increased faster and the difference in viability was slightly smaller than in KG-1a cells (Figure 2E). In addition, flow cytometric analysis with annexin V–PI dual staining revealed that treatment with ETP induced fewer apoptotic or dead cells in Kpm/Lats2-knockdown KG-1a cells than in control cells (Figure S2). Similar results were obtained with KG-1a cells transduced with microRNA-373,[52] which is known to down-regulate Kpm/Lats2 or those transfected with Kpm/Lats2-specific siRNA, although these reagents down-regulated Kpm/Lats expression less efficiently than the shRNA-expressing retrovirus vector (Figure S3A,B). These results clearly indicate that down-regulation of Kpm/Lats2 renders leukemic cells resistant to DNA damage.

### Down-regulation of Kpm/Lats2 inhibits transcriptional induction of p21 and PUMA without affecting the IAP family members

We next examined the expression of several key molecules involved in cell survival. We searched for those genes whose expression level in Kpm/Lats2-knockdown KG-1a cells was significantly different from that in control cells after DNA damage stress. Two genes, p21 and PUMA, were identified by real-time PCR analysis–based screening. The expressions of p21 and PUMA were clearly induced by DNA damage–inducing agents in control KG-1a cells, although KG-1a line was p53 null,[53] whereas their inductions were strongly inhibited in Kpm/Lats2-knockdown KG-1a cells (Figure 3A). This finding was also confirmed at the protein level (Figure S4). Since p21 induces cell-cycle arrest[54] and PUMA can make Bax localize onto mitochondrial membrane to trigger apoptosis,[55,56] these results seemed to be in agreement with what we observed in cell viability assay. On the other hand, none of the members of the IAP family, the major inhibitors of apoptosis,[57] was up-regulated by silencing of Kpm/Lats2 despite treatment with ETP (Figure 3B). Of note is that in *Drosophila* the Hippo signals end up with the inhibition of Yki leading to apoptosis via down-regulation of Diap1.[7] In addition, although Bcl-2 was reportedly decreased by ectopic expression of Kpm/Lats2,[22] there was no significant difference in its expression level between Kpm/Lats2-knockdown and control cells (Figure 3B).

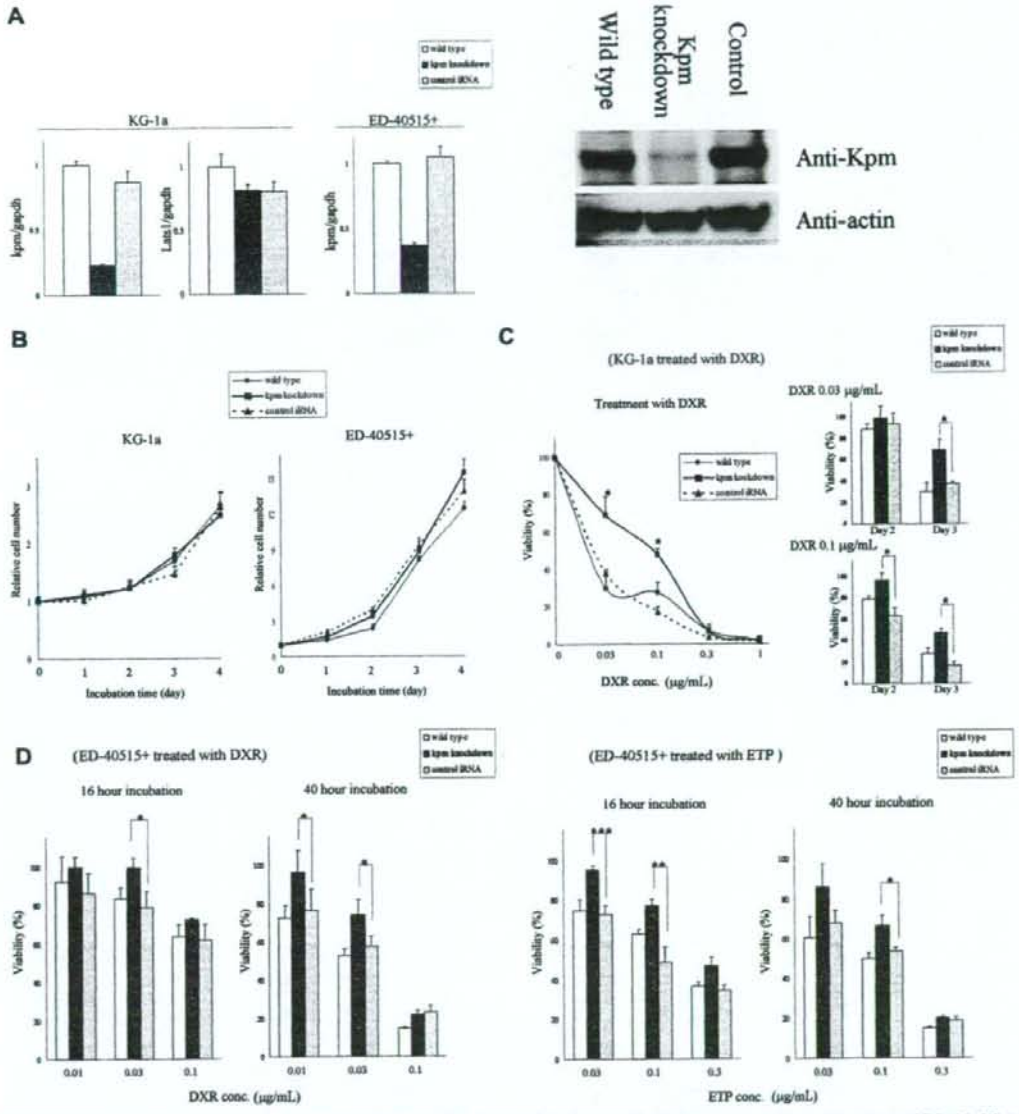


**Figure 2. Down-regulation of Kpm/Lats2 renders cells resistant to DNA damage–inducing agents.** (A) Kpm/Lats2-knockdown cells were established in KG-1a or ED-40515$^+$ cells using retrovirus (RV) vector containing Kpm/Lats2-specific shRNA. Wild type represents non–RV-transduced cells and control iRNA represents control shRNA-containing RV–transduced cells. Efficiency of Kpm/Lats2-specific shRNA was measured by real-time PCR analyses. Data normalized to gapdh are shown as mean plus or minus SD in scale that the value for wild type is 1. Analyses were performed in triplicate independently twice and representative data are shown. Western blot analysis of Kpm/Lats2 in wild-type, knockdown, or control cells in KG-1a. Analyses were performed independently twice and representative data are shown. (B) Simple growth curve without agents was measured by MTT assay. The assays were performed in quadruplicate independently 3 times and representative data are shown as mean plus or minus SD. (C) Cell viability after treatment with doxorubicin (DXR) or etoposide (ETP) in each KG-1a line was measured by MTT assay. The assays were performed in quadruplicate independently 3 times and representative data are shown as mean plus or minus SD (Welch *t* test: $^*P < .01$; $^{**}P < .05$). (D) Cell viability after treatment with DXR or ETP in each ED-40515$^+$ line was measured by MTT assay (Welch *t* test: $^*P < .05$; $^{**}P < .01$; $^{***}P < .005$). The assays were performed independently in quadruplicate 3 times, and representative data are shown as mean plus or minus SD.

### Nuclear accumulation of p73 was suppressed in Kpm/Lats2-knockdown cells

We considered p73 as a molecule that replaced p53 in p53-null cells such as KG-1a and ED-40515$^+$ because p73 is a homologue of p53 and a transcriptional factor for p21 and PUMA expression. Therefore, we measured the amount of p73 at the protein level by Western blot analysis of whole-cell lysates. p73 was hardly detectable under normal conditions but became visible in control cells after treatment with ETP. In contrast, such increase in p73 protein was not observed in Kpm/Lats2-knockdown cells after the same treatment (Figure 4A). There was little

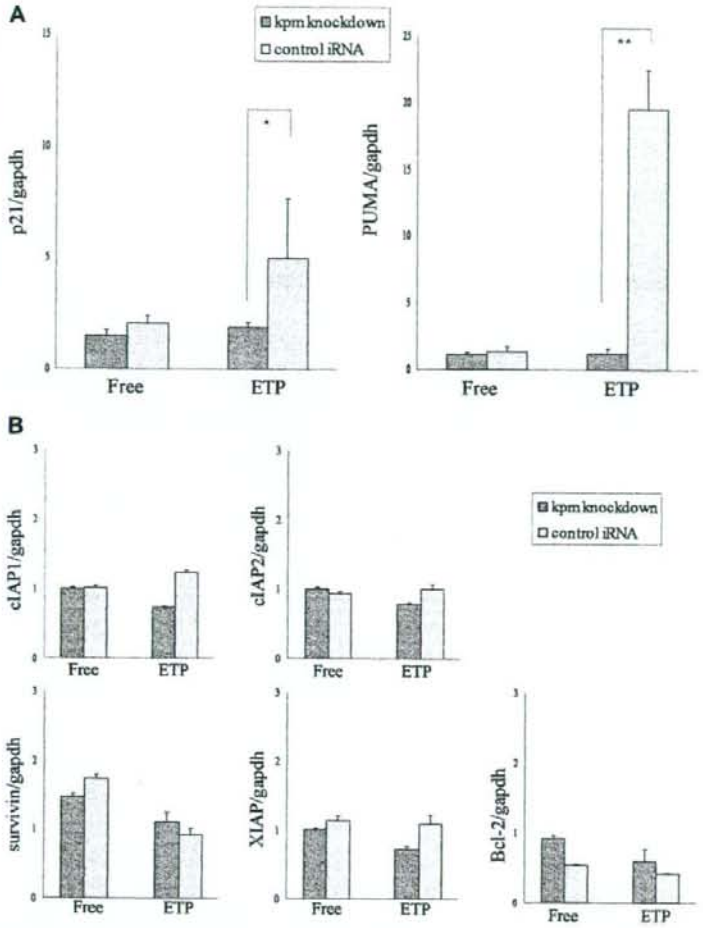


**Figure 3. Induction of p21$^{WAF1}$ and PUMA but not the IAP family members or bcl-2 is repressed in Kpm/Lats2-knockdown KG-1a cells after treatment with DNA damage–inducing agents.** Total mRNA was isolated from Kpm/Lats2-knockdown KG-1a or control cells treated with or without 0.03 μg/mL ETP at day 0 and cultured for 3 days. mRNA expression levels of p21 and PUMA (A), and the IAP family members and bcl-2 (B), were measured by real-time PCR analysis using the specific primers described in Table 1. Data normalized to gapdh are shown as mean plus or minus SD in scale that the value for KG-1a wild-type cells without treatments is 1. Normalization to hprt gave similar results. The analyses were performed in triplicate independently twice, and representative data are shown (Student *t* test: $^*P < .05$; $^{**}P < .005$).

difference in the expression level of p73 mRNA after treatment with ETP between Kpm/Lats2-knockdown cells and control cells (Figure 4B). Similar results were obtained with microRNA-373–transduced KG-1a cells (Figure S5). Next, we evaluated the distribution of p73 protein by immunofluorescence microscopy because transcriptional activity of p73 depends on the accumulation of p73 in nucleus due to posttranscriptional modification.[58] p73 was scarcely detected in KG-1a cells with or without silencing of Kpm/Lats2 under normal conditions (data not shown) but was significantly induced in control KG-1a cells after treatment with ETP (Figure 4C). In contrast, p73 remained at very low levels in Kpm/Lats2-knockdown KG-1a cells (Figure 4C). Under higher magnification, we visualized more clearly that p73, which should accumulate in the nucleus, was hardly detected or only faintly represented in Kpm/Lats2-knockdown cells (Figure 4C). Moreover, we investigated the recruitment of p73 on the *PUMA* gene promoter after DNA-damage stress. ChIP assay clearly showed that p73 was recruited to the *PUMA* gene promoter in control cells but not in Kpm/Lats2-knockdown cells after DNA-damage stress (Figure 4D). In summary, our data suggest that Kpm/Lats2 contributes to the stability of p73 protein, which in turn leads to transcriptional induction of p21 and PUMA to finally trigger cell death after treatment with DNA damage–inducing reagents.

### Kpm/Lats2 can associate with YAP2 via the first WW domain and induce its phosphorylation

We investigated whether Kpm/Lats2 could interact with and phosphorylate YAP as demonstrated in *Drosophila*. YAP has 2 major functional isoforms, YAP1 and YAP2, and we found that YAP2 was a dominant form expressed in hematopoietic lineage cells (Figure S2). Coimmunoprecipitation analyses indicated that Kpm/Lats2 interacted with YAP2 via its first WW domain (Figure 5A) and YAP1 via its only WW domain (Figure S5). In addition, coexpression of Kpm/Lats2 and YAP2 resulted in a mobility shift of YAP2. This mobility shift was abrogated by phosphatase treatment and was not caused by coexpression of the Kpm-kinase–dead form and YAP2. Therefore, this shift is indeed due to the phosphorylation of YAP protein (Figure 5B). It was unexpected, however, that this mobility shift occurred with the first WW domain mutant but not with the S127A mutant form of YAP2. Phosphorylation of YAP2 at serine 127 was further confirmed by Western blot using anti–phospho-YAP, which could recognize phosphorylated serine 127 of YAP2 specifically. In accordance with mobility shift assay, the phosphorylated YAP2 was clearly detected in coexpression of wild-type Kpm/Lats2 but barely detectable in coexpression of

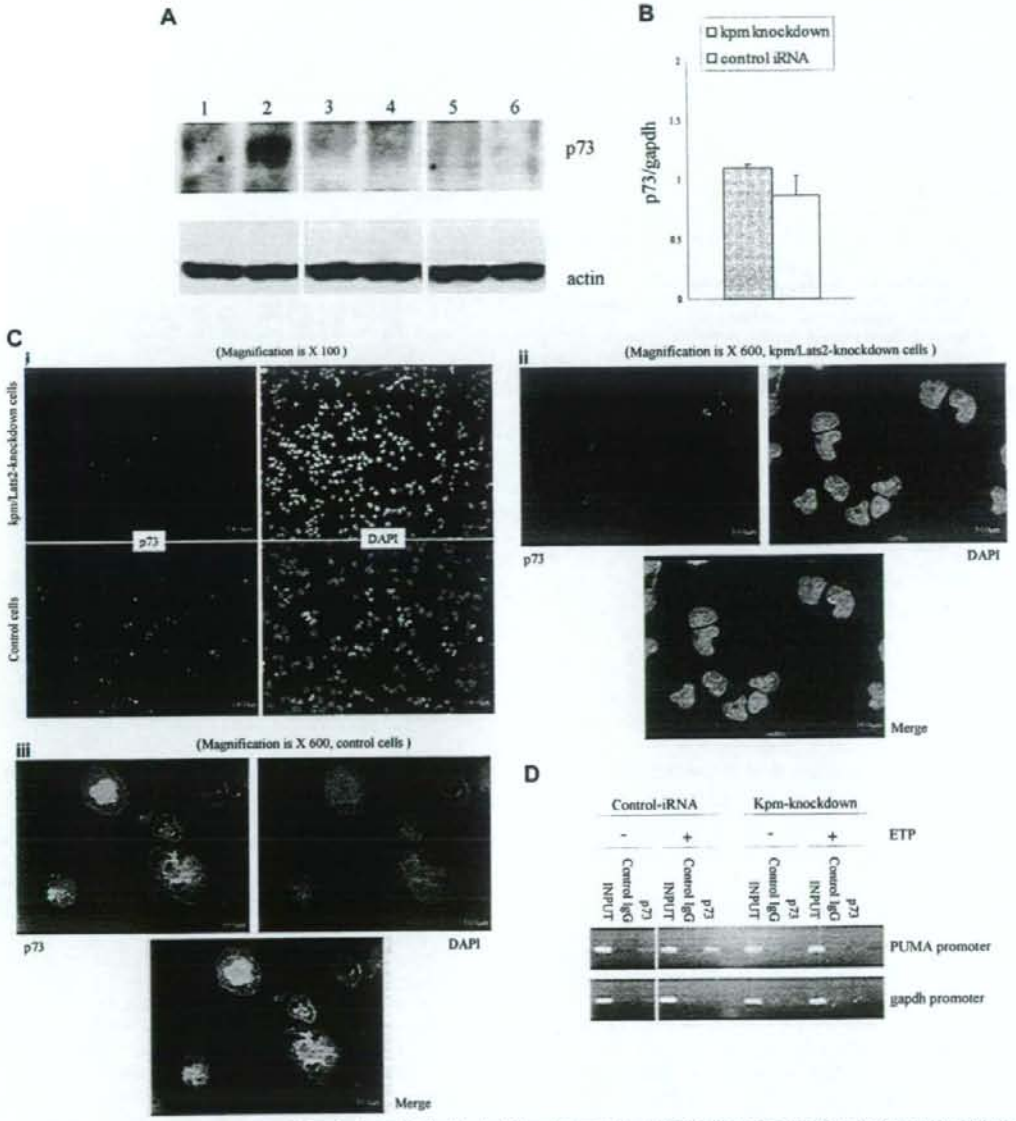


**Figure 4. Stabilization of p73 after treatment with ETP is insufficient in Kpm/Lats2-knockdown cells.** (A) Western blotting analysis with anti-p73 in whole-cell lysate of control KG-1a cells without treatment of ETP (lane 1) or with treatment of 0.03 μg/mL ETP for 3 days (lane 2), Kpm/Lats2-knockdown KG-1a cells without treatment of ETP (lane 3), or with treatment of 0.03 μg/mL ETP for 3 days (lane 4), and p73-knockdown KG-1a cells without treatment of ETP (lane 5) or with treatment of 0.03 μg/mL ETP for 3 days (lane 6). Twice, independent experiments were performed and representative data are shown. (B) Expression of p73 mRNA in Kpm/Lats2-knockdown KG-1a or control cells treated with 0.03 μg/mL ETP for 3 days was measured by real-time PCR analysis. Data normalized to gapdh are shown as mean plus or minus SD in scale that the value for KG-1a wild-type cells with the same treatment is 1. The analyses were performed in triplicate independently twice and representative data are shown as mean plus or minus SD. (C) Immunofluorescence staining for p73 and DAPI. Kpm/Lats2-knockdown KG-1a cells and control cells treated with 0.1 μg/mL ETP were stained with anti-p73 Ab or DAPI and observed with a fluorescence microscope at the magnification of ×100 or ×600. Four independent experiments were performed and representative data are shown. (D) ChIP assay. ChIP assay was performed as described in "Chromatin immunoprecipatation assay." p73 was recruited to *PUMA* gene promoter in control cells but not in Kpm/Lats2-knockdown cells after the treatment with 0.03 μg/mL ETP for 60 hours. Two independent experiments were performed and representative data are shown.

kinase-dead form of Kpm/Lats2 or mock. It was also detected in coexpression of wild-type of Kpm/Lats2 with first WW domain mutant or second WW domain mutant of YAP2. These data suggest that Kpm/Lats2 phosphorylates YAP2 at serine 127 regardless of interaction via the WW domains.

### Stabilization of p73 requires YAP2 and kinase activity of Kpm

Finally, we addressed how the interaction between Kpm/Lats2 and YAP2 contributes to stabilization of p73. p73 was cotransfected with wild type as well as mutant clones of Kpm/Lats2 and YAP2 into 293T

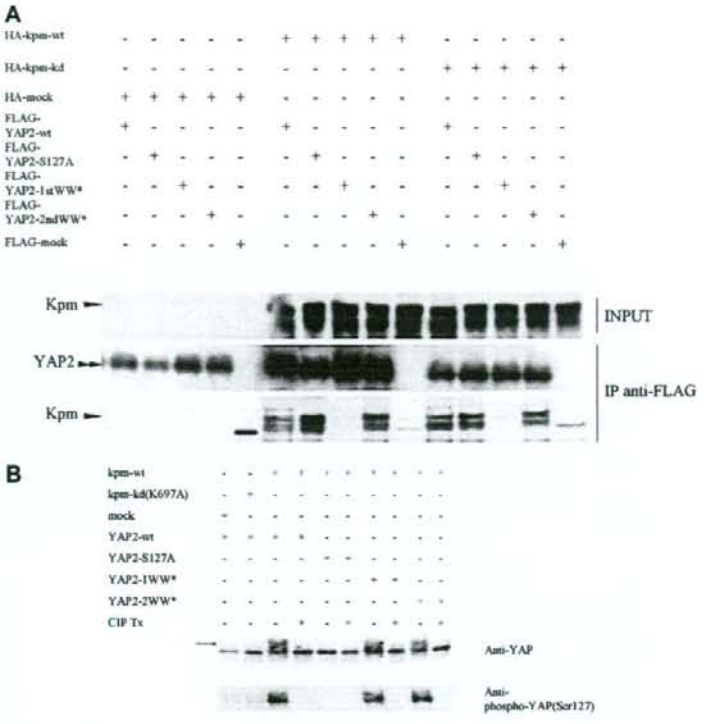


**Figure 5. Kpm/Lats2 can associate with YAP2 via its first WW domain and phosphorylate YAP2, but it requires not this association but kinase function of Kpm/Lats2 to stabilize p73.** (A) Any one of HA-tagged Kpm-wild type (wt), Kpm-kinase dead (kd), or mock was cotransfected with any one of FLAG-tagged YAP2-wild type (wt), YAP2-S127A (mutant form S127 to A; S127 is Akt-phosphorylation site), YAP2-1WW* (mutant form of first WW domain), YAP2-2WW* (mutant form of second WW domain), or mock into 293T cells by the calcium phosphate method. Upper lanes represent Western blotting with anti-HA in cell lysates. Middle lanes and lower lanes represent Western blotting with anti-FLAG and anti-HA, respectively, in the immunoprecipitates by anti-FLAG. Three independent experiments were performed and representative data are shown. (B) The coimmunoprecipitate fraction by anti-FLAG from each lysate was treated with or without CIP and then analyzed by Western blotting with anti-YAP polyclonal antibody and anti–phospho-YAP (Ser127) polyclonal antibody. Arrow indicates mobility shift band of YAP2. Three independent experiments were performed and representative data are shown.

cells, and the protein levels of these molecules were estimated by Western blot. These transient coexpression experiments showed that the protein level of p73 was high in coexpression of wild-type YAP2 and wild-type Kpm/Lats2 but not the kinase-dead form or mock. High expression of p73 was observed not only in coexpression of the second WW domain mutant of YAP2 that was able to interact with Kpm/Lats2 but also in that of the first WW domain mutant of YAP2 that was unable to do that. On the other hand, the expression level of p73 was not increased in coexpression of the S127A mutant of YAP2 compared with mock. Furthermore, coexpression of wild-type Kpm/Lats2 but not the kinase-dead form augmented the protein level of YAP2 regardless of the presence of the first WW domain, and even wild-type Kpm/Lats2 did not affect the protein level of the S127A mutant of YAP2 (Figure 6). Similar results were obtained in the experiments of coexpression of Kpm/Lats2 and YAP1 (Figure S6). Considering that YAP is an important cofactor that associates with and stabilizes p73, the increase in p73 expression may be due to its stabilization by facilitated interaction with YAP2 mediated by its phosphorylation by Kpm/Lats2. Overall, these findings suggest that Kpm/Lats2 is involved in the stabilization of p73 by increasing the protein level of YAP2, which is dependent on the serine 127 of YAP2 and the kinase function of Kpm/Lats2.

## Discussion

*Drosophila* Warts/Lats is considered to be a tumor suppressor since its loss of function mutation results in overproliferation phenotype in mosaic animals.[1,2] The equivalent experiment has not been reproduced with Kpm/Lats2 in mammals because Kpm/Lats2 knockout mice are embryonically lethal.[26,27] Nevertheless, down-regulation of Kpm/Lats2 has been described in a variety of human cancers.[42,43,59] Notably, low level of Kpm/Lats2 expression correlated with poor prognosis in ALL.[43] Therefore, we focused on the cellular changes caused by down-regulation of Kpm/Lats2 expression. The most intriguing finding was that silencing of Kpm/Lats2 in 2 types of leukemic cells resulted in increased resistance to DNA damage–inducing agents. The viability of Kpm/Lats2-knockdown KG-1a cells after treatment with ETP or DXR was consistently higher than that of wild-type or control cells. This tendency was also observed in Kpm/Lats2-knockdown ED-40515$^+$ cells. Based on the findings of Hippo pathway in *Drosophila*, we expected that a direct executor may be one of the IAP family members because IAPs are major inhibitor of caspases, but the mRNA expression levels of IAP family members were not altered in Kpm/Lats2-knockdown cells. To find out what molecules could directly cause such resistance, we used real-time PCR analysis to search for altered expression of several candidate genes related to cell-cycle arrest or apoptosis. Among the candidates we screened, induction of p21 and PUMA by treatment with ETP was markedly suppressed in Kpm/Lats2-knockdown cells compared with control shRNA-transduced cells that responded with high levels of these genes. p21 is a well-known CDK inhibitor that induces cell cycle arrest,[60] and PUMA is a final executor that localizes BAX onto mitochondrial membrane to trigger apoptosis.[56] Therefore, the suppressed induction of these genes in Kpm/Lats2-knockdown KG-1a cells seems to be compatible with their resistance to DNA damage–inducing agents.

Expression of both p21 and PUMA is induced by p53 and its family members. Since KG-1a cells[53] and ED-40515$^+$ cells are p53 null (Dr M. Matsuoka, Kyoto University, e-mail communication,

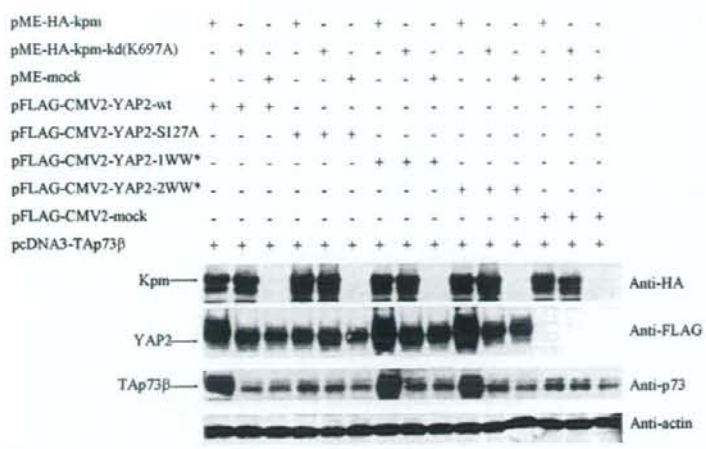


**Figure 6. The protein level of p73 is increased by coexpression of YAP2 and wild-type Kpm/Lats2.** Any one of HA-tagged Kpm-wild type (wt), Kpm-kinase dead (kd), or mock was cotransfected with TAp73α and any one of FLAG-tagged YAP2-wt, YAP2-S127A, YAP2-1WW*, YAP2-2WW*, or mock into 293T cells by FuGENE-HD reagent. Four rows of lanes from the top in this order represent Western blotting with anti-HA, anti-FLAG, anti-p73, and antiactin in cell lysates. Two independent experiments were performed and representative data are shown.

April 16, 2007), we thought that another p53 family member, presumably transcriptionally active p73 (TAp73), should function in the induction of p21 and PUMA in these cells. p73 is able to bind promoters of several p53 responsible genes involved in cell cycle arrest and apoptosis including p21 and PUMA.[61] Unlike p53, it is rarely mutated or deleted in human malignant cells.[62,63] In addition, it has been reported that knockdown of p73 leads to enhanced resistance to DNA damage–inducing agents including DXR, ETP, and cisplatinum.[64] Protein levels of p73 are kept low due to rapid degradation through the ubiquitin pathway under physiological conditions,[65] whereas TAp73 accumulates in response to stress caused by DNA damage.[66] Therefore, we regarded p73 as a p53-substituting molecule that mediated induction of p21 and PUMA, and examined the amount and the distribution of p73 in Kpm/Lats2-knockdown KG-1a cells and in control cells after treatment with ETP. As expected, after treatment of ETP, p73 protein level was kept very low in Kpm/Lats2-knockdown KG-1a cells compared with control cells, despite no difference in the mRNA level of p73. Immunofluorescence microscopic analysis revealed that nuclear accumulation of p73 was clearly detected in control cells but not, or only faintly, in Kpm/Lats2-knockdown cells. These results suggest that Kpm/Lats2 is involved in the stability and the nuclear accumulation of p73.

It has been shown that several steps are required for DNA damage–induced activation and stabilization of p73. DNA damage induces p73 gene expression via Chk1,[67] Chk2,[68] and E2F1,[69,70] and in parallel activates c-Abl and p38 MAP kinase (MAPK). Activated c-Abl and p38 MAPK phosphorylates p73 at Tyr99 and at Ser/Thr-Pro, respectively, to stabilize it in the nucleus.[71-74] In addition to phosphorylation, binding of phosphorylated p73 to promyelocytic leukemia protein (PML),[65] acetylation of p73 mediated by p300,[75] and prolyl isomerization of p73 mediated by peptidyl-prolyl *cis/trans* isomerase Pin1[76] are essential for functional activation of p73. YAP is essential for coactivation of p73 with PML and for recruitment of p300 and contributes to the DNA damage–induced nuclear accumulation of p73. Trapping of YAP in the cytosol due to phosphorylation by Akt (protein kinase B) and binding to 14-3-3 represents a physiological mechanism for the inhibition of inappropriately accumulated p73.[77,78] Among these factors, we concentrated our efforts on YAP because it should mediate the downstream signals of Kpm/Lats2 based on the analogy of *Drosophila*. We confirmed that Kpm/Lats2 could interact with YAP2 through its first WW domain and induce phosphorylation of YAP2, which indicates that the Hpo-Wts-Yki axis is evolutionally conserved. However, the downstream signals of YAP (Yki) in mammals may be different from that in *Drosophila*, because, as mentioned in "Introduction," YAP has dual and opposite functions, growth-promoting or proapoptotic. In addition, as shown in this study, no alterations of the IAP family members were detected in Kpm/Lats-knockdown cells, although Diap1 is considered to be one of the final target molecules in the *Drosophila* Hippo pathway. There is no report describing YAP-dependent regulation of the IAP family members in mammalian cells.

With regard to the relationship among Kpm/Lats2, YAP2, and p73, the transient expression experiments suggested that coexpression of Kpm/Lats2 positively regulates the protein amounts of both YAP2 and p73 in whole-cell lysates regardless of interaction with YAP2 via the WW domains and this effect requires phosphorylation of YAP2 at serine 127 by Kpm/Lats2. After submission of our original paper, Matallanas et al have reported that RASSF1A activates Lats1 through enhanced phosphorylation by MST2 and activated Lats1 phosphorylates and activates YAP1, allowing YAP1 to translocate to the nucleus and associate with p73, resulting in transcription of the proapoptotic target gene PUMA.[79] According to the authors, phosphorylation of YAP1 by Lats1 is needed to enable the formation of a YAP1-p73 complex, whereas, in unstimulated cells, Lats1 can negatively regulate YAP1 by sequestering YAP1 in the cytosol. Thus, it is suggested that Lats1 has dual functions as an anchoring protein that retains YAP1 in the cytosol and as a kinase that phosphorylates YAP1 to facilitate its interaction with p73. The former function has been emphasized by 2 recent papers insisting that inactivation of YAP by the Hippo pathway is involved in organ size control and cell contact inhibition.[80,81] These papers describe that Lats1 or Kpm/Lats2 but not AKT directly phosphorylates YAP at serine 127, increasing the interaction between YAP2 and 14-3-3. Our results are compatible with those with RASSF1A activation in that Lats1 or Kpm/Lats2 is crucial for the induction of proapoptotic gene PUMA that is mediated by the YAP-p73 complex. It should be noted that such function of Lats1 or Kpm/Lats2 becomes dominant only in the presence of proapoptotic stimulations such as RASSF1A activation, anti-Fas, and DNA damage–inducing agents. Evidence has indicated that DNA damage stress induces activation of c-Jun N-terminal kinase (JNK) and activated JNK then phosphorylates 14-3-3, resulting in release of

several 14-3-3–binding proteins including c-Abl, which is known to activate and stabilize p73 in the nucleus.[82,83] Thus, it seems possible that phosphorylation of 14-3-3 by activated JNK is involved in Kpm/Lats2-dependent nuclear translocation of YAP and accumulation of the YAP-p73 complex after DNA damage. Further studies are needed to clarify how DNA damage signals intersect the Hippo pathway.

In conclusion, we demonstrate that Kpm/Lats2 is required for the stabilization of p73 and subsequent induction of p21 and PUMA in response to DNA damage–inducing agents, suggesting that the down-regulation of Kpm/Lats2 contributes to the instability of p73 through the insufficient phosphorylation of YAP2 at serine 127, resulting in chemoresistance and poor prognosis for some leukemias.

## Acknowledgments

We thank Dr Masao Matsuoka and Dr Michiyuki Maeda (Laboratory of Virus Immunology, Research Center for AIDS, Institute for Virus Research, Kyoto University) for ATL-derived cell lines and the personal communication concerning ED-40515$^+$; Dr Akira Nakagawara and Dr Toshinori Ozaki (Biochemistry, Chiba Cancer Center Research Institute, Chiba, Japan) for their experimental advice on p73; Dr Syohei Yamaoka for his help in preparation of retrovirus vectors; Dr Yoshihide Ueda (Department of Gastroenterology and Hepatology, Kyoto University) for TAp73α; Virginia Mazack for expert technical assistance; and Dr Akifumi Takaori-Kondo (Department of Hematology and Oncology, Kyoto University) for the immunofluorescence microscope and his continuous help.

This work was supported in part by grants-in-aid from the Ministry of Education, Culture, Sports, Science, and Technology of Japan (T.H. and T.U.), and by a Pennsylvania Department of Health–sponsored Breast Cancer Research Grant (Philadelphia, PA; SAP no. 41-000-37378, M.S.).

## Authorship

Contribution: M.K. performed most experiments and cowrote the paper; T.H. designed the research and cowrote the paper; K.C. performed some experiments; T.O. and M.S. contributed vital plasmids; and T.U. supervised the research.

Conflict-of-interest disclosure: The authors declare no competing financial interests.

Correspondence: Toshiyuki Hori, Department of Hematology and Oncology, Graduate School of Medicine, Kyoto University, 54 Shogoin-Kawara-cho, Sakyo-ku, Kyoto 606-8507, Japan; e-mail: thori@kuhp.kyoto-u.ac.jp.

## References

1. Justice RW, Zilian O, Woods DF, Noll M, Bryant PJ. The Drosophila tumor suppressor gene warts encodes a homolog of human myotonic dystrophy kinase and is required for the control of cell shape and proliferation. Genes Dev. 1995;9:534-546.
2. Xu T, Wang W, Zhang S, Stewart RA, Yu W. Identifying tumor suppressors in genetic mosaics: the Drosophila lats gene encodes a putative protein kinase. Development. 1995;121:1053-1063.
3. Edgar BA. From cell structure to transcription: Hippo forges a new path. Cell. 2006;124:267-273.
4. Harvey K, Tapon N. The Salvador-Warts-Hippo pathway: an emerging tumour-suppressor network. Nat Rev Cancer. 2007;7:182-191.
5. Pan D. Hippo signaling in organ size control. Genes Dev. 2007;21:886-897.
6. Harvey KF, Pfleger CM, Hariharan IK. The Drosophila Mst ortholog, hippo, restricts growth and cell proliferation and promotes apoptosis. Cell. 2003;114:457-467.
7. Huang J, Wu S, Barrera J, Matthews K, Pan D. The Hippo signaling pathway coordinately regulates cell proliferation and apoptosis by inactivating Yorkie, the Drosophila Homolog of YAP. Cell. 2005;122:421-434.
8. Tapon N, Harvey KF, Bell DW, et al. salvador promotes both cell cycle exit and apoptosis in Drosophila and is mutated in human cancer cell lines. Cell. 2002;110:467-478.
9. Wu S, Huang J, Dong J, Pan D. hippo encodes a Ste-20 family protein kinase that restricts cell proliferation and promotes apoptosis in conjunction with salvador and warts. Cell. 2003;114:445-456.
10. He Y, Emoto K, Fang X, et al. Drosophila Mob family proteins interact with the related tricornered (Trc) and warts (Wts) kinases. Mol Biol Cell. 2005;16:4139-4152.
11. Lai ZC, Wei X, Shimizu T, et al. Control of cell proliferation and apoptosis by mob as tumor suppressor, mats. Cell. 2005;120:675-685.
12. Wei X, Shimizu T, Lai ZC. Mob as tumor suppressor is activated by Hippo kinase for growth inhibition in Drosophila. EMBO J. 2007;26:1772-1781.
13. Hamaratoglu F, Willecke M, Kango-Singh M, et al. The tumour-suppressor genes NF2/Merlin and Expanded act through Hippo signalling to regulate cell proliferation and apoptosis. Nat Cell Biol. 2006;8:27-36.
14. Bennett FC, Harvey KF. Fat cadherin modulates organ size in Drosophila via the Salvador/Warts/Hippo signaling pathway. Curr Biol. 2006;16:2101-2110.
15. Cho E, Feng Y, Rauskolb C, Maitra S, Fehon R, Irvine KD. Delineation of a Fat tumor suppressor pathway. Nat Genet. 2006;38:1142-1150.
16. Silva E, Tsatskis Y, Gardano L, Tapon N, McNeill H. The tumor-suppressor gene fat controls tissue growth upstream of expanded in the hippo signaling pathway. Curr Biol. 2006;16:2081-2089.
17. Willecke M, Hamaratoglu F, Kango-Singh M, et al. The fat cadherin acts through the hippo tumor-suppressor pathway to regulate tissue size. Curr Biol. 2006;16:2090-2100.
18. Hori T, Takaori-Kondo A, Kamikubo Y, Uchiyama T. Molecular cloning of a novel human protein kinase, kpm, that is homologous to warts/lats, a Drosophila tumor suppressor. Oncogene. 2000;19:3101-3109.
19. Yabuta N, Fujii T, Copeland NG, et al. Structure, expression, and chromosome mapping of LATS2, a mammalian homologue of the Drosophila tumor suppressor gene lats/warts. Genomics. 2000;63:263-270.
20. Kamikubo Y, Takaori-Kondo A, Uchiyama T, Hori T. Inhibition of cell growth by conditional expression of kpm, a human homologue of Drosophila warts/lats tumor suppressor. J Biol Chem. 2003;278:17609-17614.
21. Li Y, Pei J, Xia H, Ke H, Wang H, Tao W. Lats2, a putative tumor suppressor, inhibits G1/S transition. Oncogene. 2003;22:4398-4405.
22. Ke H, Pei J, Ni Z, et al. Putative tumor suppressor Lats2 induces apoptosis through downregulation of Bcl-2 and Bcl-x(L). Exp Cell Res. 2004;298:329-338.
23. Aylon Y, Michael D, Shmueli A, Yabuta N, Nojima H, Oren M. A positive feedback loop between the p53 and Lats2 tumor suppressors prevents tetraploidization. Genes Dev. 2006;20:2687-2700.
24. Kostic C, Shaw PH. Isolation and characterization of sixteen novel p53 response genes. Oncogene. 2000;19:3978-3987.
25. Colombani J, Polesello C, Josue F, Tapon N. Dmp53 activates the Hippo pathway to promote cell death in response to DNA damage. Curr Biol. 2006;16:1453-1458.
26. McPherson JP, Tamblyn L, Elia A, et al. Lats2/Kpm is required for embryonic development, proliferation control and genomic integrity. EMBO J. 2004;23:3677-3688.
27. Yabuta N, Okada N, Ito A, et al. Lats2 is an essential mitotic regulator required for the coordination of cell division. J Biol Chem. 2007;282:19259-19271.
28. Chan EH, Nousiainen M, Chalamalasetty RB, Schafer A, Nigg EA, Sillje HH. The Ste20-like kinase Mst2 activates the human large tumor suppressor kinase Lats1. Oncogene. 2005;24:2076-2086.
29. Sudol M. Yes-associated protein (YAP65) is a proline-rich phosphoprotein that binds to the SH3 domain of the Yes proto-oncogene product. Oncogene. 1994;9:2145-2152.
30. Sudol M, Bork P, Einbond A, et al. Characterization of the mammalian YAP (Yes-associated protein) gene and its role in defining a novel protein module, the WW domain. J Biol Chem. 1995;270:14733-14741.
31. Macias MJ, Wiesner S, Sudol M. WW and SH3 domains, two different scaffolds to recognize proline-rich ligands. FEBS Lett. 2002;513:30-37.
32. Vassilev A, Kaneko KJ, Shu H, Zhao Y, DePamphilis ML. TEAD/TEF transcription factors utilize the activation domain of YAP65, a Src/Yes-associated protein localized in the cytoplasm. Genes Dev. 2001;15:1229-1241.
33. Komuro A, Nagai M, Navin NE, Sudol M. WW domain-containing protein YAP associates with ErbB-4 and acts as a co-transcriptional activator for the carboxyl-terminal fragment of ErbB-4 that translocates to the nucleus. J Biol Chem. 2003;278:33334-33341.

34. Aqeilan RI, Donati V, Palamarchuk A, et al. WW domain-containing proteins, WWOX and YAP, compete for interaction with ErbB-4 and modulate its transcriptional function. Cancer Res. 2005;65: 6764-6772.
35. Yagi R, Chen LF, Shigesada K, Murakami Y, Ito Y. A WW domain-containing yes-associated protein (YAP) is a novel transcriptional co-activator. EMBO J. 1999;18:2551-2562.
36. Zaidi SK, Sullivan AJ, Medina R, et al. Tyrosine phosphorylation controls Runx2-mediated subnuclear targeting of YAP to repress transcription. EMBO J. 2004;23:790-799.
37. Overholtzer M, Zhang J, Smolen GA, et al. Transforming properties of YAP, a candidate oncogene on the chromosome 11q22 amplicon. Proc Natl Acad Sci U S A. 2006;103:12405-12410.
38. Zender L, Spector MS, Xue W, et al. Identification and validation of oncogenes in liver cancer using an integrative oncogenomic approach. Cell. 2006;125:1253-1267.
39. Espanel X, Sudol M. Yes-associated protein and p53-binding protein-2 interact through their WW and SH3 domains. J Biol Chem. 2001;276:14514-14523.
40. Samuels-Lev Y, O'Connor DJ, Bergamaschi D, et al. ASPP proteins specifically stimulate the apoptotic function of p53. Mol Cell. 2001;8:781-794.
41. Dobbelstein M, Strano S, Roth J, Blandino G. p73-induced apoptosis: a question of compartments and cooperation. Biochem Biophys Res Commun. 2005;331:688-693.
42. Takahashi Y, Miyoshi Y, Takahata C, et al. Down-regulation of LATS1 and LATS2 mRNA expression by promoter hypermethylation and its association with biologically aggressive phenotype in human breast cancers. Clin Cancer Res. 2005; 11:1380-1385.
43. Jiménez-Velasco A, Roman-Gomez J, Agirre X, et al. Downregulation of the large tumor suppressor 2 (LATS2/KPM) gene is associated with poor prognosis in acute lymphoblastic leukemia. Leukemia. 2005;19:2347-2350.
44. Koeffler HP, Billing R, Lusis AJ, Sparkes R, Golde DW. An undifferentiated variant derived from the human acute myelogenous leukemia cell line (KG-1). Blood. 1980;56:265-273.
45. Maeda M, Arima N, Daitoku Y, et al. Evidence for the interleukin-2 dependent expansion of leukemic cells in adult T cell leukemia. Blood. 1987;70: 1407-1411.
46. Ohno Y, Amakawa R, Fukuhara S, et al. Acute transformation of chronic large granular lymphocyte leukemia associated with additional chromosome abnormality. Cancer. 1989;64:63-67.
47. Kawahara M, Hori T, Matsubara Y, Okawa K, Uchiyama T. Identification of HLA class I-restricted tumor-associated antigens in adult T cell leukemia cells by mass spectrometric analysis. Exp Hematol. 2006;34:1496-1504.
48. Matsubar Y, Hori T, Morita R, Sakaguchi S, Uchiyama T. Delineation of immunoregulatory properties of adult T-cell leukemia cells. Int J Hematol. 2006;84:63-69.
49. Ueda Y, Hijikata M, Takagi S, Chiba T, Shimotohno K. New p73 variants with altered C-terminal structures have varied transcriptional activities. Oncogene. 1999;18:4993-4998.
50. National Center for Biotechnology Information. BLASTN. http://www.ncbi.nlm.nih.gov/blast/Blast.cgi?PAGE=Nucleotides&PROGRAM=blastn. Accessed on March 11, 2005.
51. Rocco JW, Leong CO, Kuperwasser N, DeYoung MP, Ellisen LW. p63 mediates survival in squamous cell carcinoma by suppression of p73-dependent apoptosis. Cancer Cell. 2006;9:45-56.
52. Voorhoeve PM, le Sage C, Schrier M, et al. A genetic screen implicates miRNA-372 and miRNA-373 as oncogenes in testicular germ cell tumors. Cell. 2006;124:1169-1181.
53. Clave E, Carosella ED, Gluckman E, Socie G. Radiation-enhanced expression of interferon-inducible genes in the KG1a primitive hematopoietic cell line. Leukemia. 1997;11:114-119.
54. Weiss RH. p21Waf1/Cip1 as a therapeutic target in breast and other cancers. Cancer Cell. 2003;4: 425-429.
55. Yu J, Zhang L. No PUMA, no death: implications for p53-dependent apoptosis. Cancer Cell. 2003; 4:248-249.
56. Kim H, Rafiuddin-Shah M, Tu HC, et al. Hierarchical regulation of mitochondrion-dependent apoptosis by BCL-2 subfamilies. Nat Cell Biol. 2006; 8:1348-1358.
57. Nachmias B, Ashhab Y, Ben-Yehuda D. The inhibitor of apoptosis protein family (IAPs): an emerging therapeutic target in cancer. Semin Cancer Biol. 2004;14:231-243.
58. Ozaki T, Nakagawara A. p73, a sophisticated p53 family member in the cancer world. Cancer Sci. 2005;96:729-737.
59. Jiang Z, Li X, Hu J, et al. Promoter hypermethylation-mediated down-regulation of LATS1 and LATS2 in human astrocytoma. Neurosci Res. 2006;56:450-458.
60. Sherr CJ, Roberts JM. Inhibitors of mammalian G1 cyclin-dependent kinases. Genes Dev. 1995; 9:1149-1163.
61. Melino G, De Laurenzi V, Vousden KH. p73: friend or foe in tumorigenesis. Nat Rev Cancer. 2002;2:605-615.
62. Ichimiya S, Nimura Y, Kageyama H, et al. p73 at chromosome 1p36.3 is lost in advanced stage neuroblastoma but its mutation is infrequent. Oncogene. 1999;18:1061-1066.
63. Pluta A, Nyman U, Joseph B, Robak T, Zhivotovsky B, Smolewski P. The role of p73 in hematological malignancies. Leukemia. 2006;20: 757-766.
64. Irwin MS, Kondo K, Marin MC, Cheng LS, Hahn WC, Kaelin WG Jr. Chemosensitivity linked to p73 function. Cancer Cell. 2003;3:403-410.
65. Bernassola F, Salomoni P, Oberst A, et al. Ubiquitin-dependent degradation of p73 is inhibited by PML. J Exp Med. 2004;199:1545-1557.
66. Rossi M, De Laurenzi V, Munarriz E, et al. The ubiquitin-protein ligase Itch regulates p73 stability. EMBO J. 2005;24:836-848.
67. Gonzalez S, Prives C, Cordon-Cardo C. p73alpha regulation by Chk1 in response to DNA damage. Mol Cell Biol. 2003;23:8161-8171.
68. Urist M, Tanaka T, Poyurovsky MV, Prives C. p73 induction after DNA damage is regulated by checkpoint kinases Chk1 and Chk2. Genes Dev. 2004;18:3041-3054.
69. Irwin M, Marin MC, Phillips AC, et al. Role for the p53 homologue p73 in E2F-1-induced apoptosis. Nature. 2000;407:645-648.
70. Stiewe T, Putzer BM. Role of the p53-homologue p73 in E2F1-induced apoptosis. Nat Genet. 2000; 26:464-469.
71. Agami R, Blandino G, Oren M, Shaul Y. Interaction of c-Abl and p73alpha and their collaboration to induce apoptosis. Nature. 1999;399:809-813.
72. Gong JG, Costanzo A, Yang HQ, et al. The tyrosine kinase c-Abl regulates p73 in apoptotic response to cisplatin-induced DNA damage. Nature. 1999;399:806-809.
73. Yuan ZM, Shioya H, Ishiko T, et al. p73 is regulated by tyrosine kinase c-Abl in the apoptotic response to DNA damage. Nature. 1999;399:814-817.
74. Sanchez-Prieto R, Rojas JM, Taya Y, Gutkind JS. A role for the p38 mitogen-acitvated protein kinase pathway in the transcriptional activation of p53 on genotoxic stress by chemotherapeutic agents. Cancer Res. 2000;60:2464-2472.
75. Costanzo A, Merlo P, Pediconi N, et al. DNA damage-dependent acetylation of p73 dictates the selective activation of apoptotic target genes. Mol Cell. 2002;9:175-186.
76. Mantovani F, Piazza S, Gostissa M, et al. Pin1 links the activities of c-Abl and p300 in regulating p73 function. Mol Cell. 2004;14:625-636.
77. Basu S, Totty NF, Irwin MS, Sudol M, Downward J. Akt phosphorylates the Yes-associated protein, YAP, to induce interaction with 14-3-3 and attenuation of p73-mediated apoptosis. Mol Cell. 2003; 11:11-23.
78. Strano S, Monti O, Pediconi N, et al. The transcriptional coactivator Yes-associated protein drives p73 gene-target specificity in response to DNA Damage. Mol Cell. 2005;18:447-459.
79. Matallanas D, Romano D, Yee K, et al. RASSF1A elicits apoptosis through an MST2 pathway directing proapoptotic transcription by the p73 tumor suppressor protein. Mol Cell. 2007;27:962-975.
80. Dong J, Feldmann G, Huang J, et al. Elucidation of a universal size-control mechanism in Drosophila and mammals. Cell. 2007;130:1120-1133.
81. Zhao B, Wei X, Li W, et al. Inactivation of YAP oncoprotein by the Hippo pathway is involved in cell contact inhibition and tissue growth control. Genes Dev. 2007;21:2747-2761.
82. Yoshida K, Yamaguchi T, Natsume T, Kufe D, Miki Y. JNK phosphorylation of 14-3-3 proteins regulates nuclear targeting of c-Abl in the apoptotic response to DNA damage. Nat Cell Biol. 2005;7: 278-285.
83. Sunayama J, Tsuruta F, Masuyama N, Gotoh Y. JNK antagonizes Akt-mediated survival signals by phosphorylating 14-3-3. J Cell Biol. 2005;170: 295-304.

# Ozone production by amino acids contributes to killing of bacteria

Kouhei Yamashita[a,1], Takashi Miyoshi[a], Toshiyuki Arai[b], Nobuyuki Endo[c], Hiroshi Itoh[d], Keisuke Makino[e], Kiyomi Mizugishi[f], Takashi Uchiyama[a], and Masataka Sasada[d]

Departments of [a]Hematology and Oncology and [b]Anesthesia, Kyoto University Hospital, Kyoto 606-8507, Japan; [c]Wakasa Wan Energy Research Center, Tsuruga, Fukui 914-0129, Japan; [d]Human Health Sciences, Graduate School of Medicine, Kyoto University, Kyoto 606-8507, Japan; [e]Institute of Advanced Energy, Kyoto University, Uji, Kyoto 611-0011, Japan; and [f]Department of Physiology, Kanazawa University Graduate School of Medical Sciences, Kanazawa, Ishikawa 920-8640, Japan

Edited by Richard A. Lerner, The Scripps Research Institute, La Jolla, CA, and approved September 18, 2008 (received for review August 12, 2008)

**Reactive oxygen species produced by phagocytosing neutrophils are essential for innate host defense against invading microbes. Previous observations revealed that antibody-catalyzed ozone formation by human neutrophils contributed to the killing of bacteria. In this study, we discovered that 4 amino acids themselves were able to catalyze the production of an oxidant with the chemical signature of ozone from singlet oxygen in the water-oxidation pathway, at comparable level to antibodies. The resultant oxidant with the chemical signature of ozone exhibited significant bactericidal activity in our distinct cell-free system and in human neutrophils. The results also suggest that an oxidant with the chemical signature of ozone produced by neutrophils might potentiate a host defense system, when the host is challenged by high doses of infectious agents. Our findings provide biological insights into the killing of bacteria by neutrophils.**

host defense | singlet oxygen | neutrophil | chronic granulomatous disease

Neutrophils are one of the professional phagocytes, which ingest microorganisms into intracellular compartments called phagosomes, and destroy them. The production of reactive oxygen species (ROS) by phagocytosing neutrophils is essential for innate host defense against invading microbial pathogens. The phagocytosing neutrophils undergo a burst of oxygen consumption that is caused by the reduced NADPH oxidase, ultimately leading to the formation of hypochlorous acid (HOCl), singlet oxygen ($^1O_2$), and hydroxyl radical ($^{\bullet}OH$). However, a clear scenario of how the ROS kill microbes has not yet emerged (1). Recently, it has been proposed that neutrophils produce ozone, which likely contributes to the bactericidal and inflammatory activity of neutrophils (2–4), although the validity of this model is still a matter of debate (5, 6). In this model, antibodies can catalyze the production of ozone from singlet oxygen and water, but the precise mechanism of how antibodies achieve this reaction remains uncertain.

Chronic granulomatous disease (CGD) is characterized by a defect in ROS formation, leading to recurrent, often life-threatening bacterial and fungal infections, and granuloma formation in multiple organs. The disease is caused by a genetic mutation in 1 of 4 components of NADPH oxidase (gp91-*phox*, p47-*phox*, p67-*phox*, and p22-*phox*) of the superoxide ($O_2^{\bullet-}$)-generating phagocytes (7). Patients with a defect in the gp91-*phox* component, which is the most common type of CGD (≈60%), are reported to exhibit a more severe clinical course than those with a defect in the p47-*phox* component (8). Recently, we experienced a patient with a rare variant type of CGD carrying a defect in the gp91-*phox* component. Despite the genetic defect, his granulocytes could produce significant amounts of singlet oxygen, but very little superoxide. Thus, neutrophils from this CGD patient would provide a useful model system in humans. In this study, we investigated the biological importance of ozone produced by human neutrophils by using the variant CGD neutrophils and our distinct in vitro assay system.

## Results

**Ozone Production by Immunoglobulins and Amino Acids in the Cell-Free System.** In our current study, we explored the mechanism by which antibodies produce ozone from singlet oxygen and water. We previously established a cell-free system, in which 6-formylpterin (6FP), a potent xanthine oxidase inhibitor, produces singlet oxygen without superoxide formation under UVA radiation in aqueous solutions (9). Using this system, we found that the portion of $F(ab')_2$ of antibodies, albumin, and chemotactic peptide, formyl-methionyl-leucyl-phenylalanine (FMLP), had the potential to generate an oxidant with the chemical signature of ozone, as intact antibodies (IgG) did, as denoted by the oxidation reaction of indigo carmine to isatin sulfonic acids, detected by a spectrophotometric assay (Fig. 1*A*). However, an inhibitory peptide of caspases, benzyloxycarbonyl-Val-Ala-Asp(OMe)-fluoromethylketone (zVAD-fmk), did not produce an oxidant with the chemical signature of ozone (Fig. 1*B*). Furthermore, the addition of catalase, which catalyzes the decomposition of $H_2O_2$ to $H_2O$ and $O_2$, did not affect the generation of an oxidant with the chemical signature of ozone by IgG in this system (Fig. 1*C*). These results substantiate the previous observation by Wentworth *et al.* (2) and further suggest that the ozone generation brought about by antibodies is not attributable to the antigen-binding activity of antibodies. We further examined what components contribute to ozone production in this system. Surprisingly, among various water-soluble amino acids applied, 4 amino acids [tryptophan (Trp), methionine (Met), cysteine (Cys), and histidine (His)] exhibited catalytic activity sufficient for the conversion of singlet oxygen to an oxidant with the chemical signature of ozone in a dose-dependent manner (Fig. 1 *D* and *E*). Scavengers of singlet oxygen, sodium azide and edaravone (10), significantly abrogated the ability of these amino acids to catalyze the reaction (Fig. 1*F*), whereas catalase had no effects on the reaction (Fig. 1*G*), suggesting the specificity of this assay system. To further verify the amino acid-catalyzed ozone generation, we performed HPLC assay for detection of isatin sulfonic acid (Fig. 2 *A* and *B*) and 4-carboxybenzaldehyde (Fig. 2 *C* and *D*). The administration of Met to 6FP under UVA radiation successfully converted indigo carmine (Fig. 2*A*) to isatin sulfonic acid (Fig. 2*B*). Moreover, another detector of ozone, vinylbenzoic acid (Fig. 2*C*), was oxidized to 4-carboxybenzaldehyde (Fig. 2*D*), support-

Author contributions: K.Y., T.U., and M.S. designed research; K.Y., T.M., T.A., N.E., and H.I. performed research; K. Makino contributed new reagents/analytic tools; K.Y. analyzed data; and K.Y. and K. Mizugishi wrote the paper.

The authors declare no conflict of interest.

This article is a PNAS Direct Submission.

[1]To whom correspondence should be addressed. E-mail: kouhei@kuhp.kyoto-u.ac.jp.

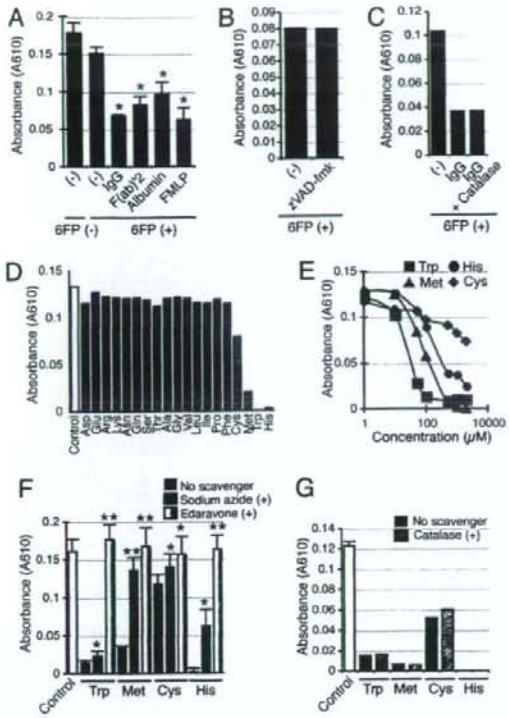


**Fig. 1.** Ozone production by immunoglobulins and amino acids in the cell-free system. Indigo carmine was irradiated with UVA in the presence of 6FP. An oxidant with the chemical signature of ozone produced by the addition of immunoglobulins or amino acids converted indigo carmine to isatin sulfonic acids. Loss of indigo carmine was monitored by measuring its absorbance at 610 nm. (*A*) Effect of Ig, the portion of $F(ab)'_2$ of antibodies, albumin, or FMLP in the presence of 6FP on ozone production. The data represent mean values ± SD ($n = 3$; *, $P < 0.05$, paired *t* test). (*B*) Effect of zVAD-fmk in the presence of 6FP on ozone production. The experiments were performed at least 3 times, and representative data are shown. (*C*) Effect of catalase in the presence of 6FP on IgG-mediated ozone production. The experiments were performed at least 3 times, and representative data are shown. (*D*) Effect of water-soluble amino acids in the presence of 6FP on ozone production. Representative data are shown. (*E*) Dose–response curves. Increasing concentrations of Trp, Met, Cys, or His (1 μM to 2 mM) were added to the reaction in the presence of 6FP. (*F*) Effect of scavengers of singlet oxygen, sodium azide, and edaravone on amino acid (Trp, Met, Cys, or His)-mediated ozone production. The data represent mean values ± SD ($n = 3$; *, $P < 0.05$; **, $P < 0.01$; paired *t* test). (*G*) Effect of catalase on amino acid (Trp, Met, Cys, or His)-mediated ozone production. The data represent mean values ± SD ($n = 3$).

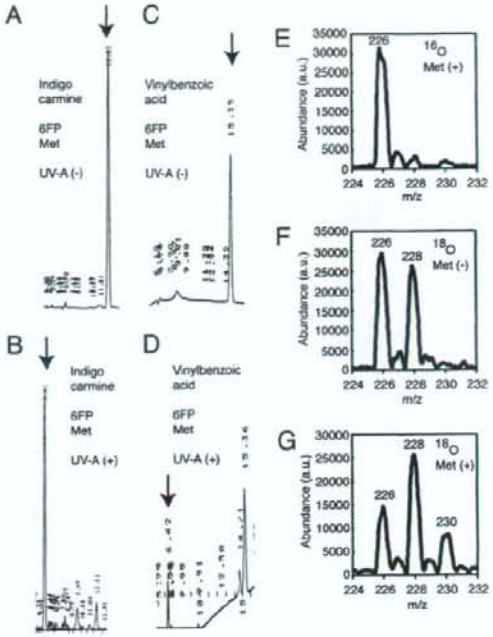


**Fig. 2.** HPLC and mass spectral analysis of ozone production in the cell-free system. (*A* and *B*) HPLC analysis. Indigo carmine was added to 6FP and Met with (*B*) or without (*A*) UVA irradiation. Arrows indicate a peak of indigo carmine (*A*) and isatin sulfonic acid (*B*). (*C* and *D*) HPLC analysis. Vinylbenzoic acid was added to 6FP and Met with (*D*) or without (*C*) UVA irradiation. Arrows indicate a peak of vinylbenzoic acid (*C*) and 4-carboxybenzaldehyde (*D*). (*E*–*G*) Mass spectral analysis. Indigo carmine was added to 6FP in a reaction mixture containing $H_2{}^{16}O$ in the presence of Met (*E*), $H_2{}^{18}O$ in the absence (*F*) or presence (*G*) of Met and irradiated with UVA. Note the presence of the mass peak 230 in *G*.

ing the formation of an oxidant with the chemical signature of ozone by amino acids. The amino acids-catalyzed ozone generation was further confirmed by measuring $^{18}O$ incorporation from the reaction solvent $H_2{}^{18}O$ into isatin sulfonic acid during indigo carmine oxidation by using mass spectral analysis. In a control experiment, where normal $H_2{}^{16}O$ was used in the presence of Met and 6FP with UVA irradiation, the mass peak 226 was detected, suggesting that isatin sulfonic acid was produced in the system (Fig. 2*E*). Mass spectral profile with $H_2{}^{18}O$ revealed that the additional mass peak 230, which is characteristic of ozone (2), was observed when Met and 6FP in a reaction mixture containing $H_2{}^{18}O$ were irradiated with UVA (Fig. 2*G*), whereas the mass peak 226 and 228 alone were observed in the absence of Met (Fig. 2*F*). These results demonstrate that the oxidant-carrying chemical signature of ozone was produced in our amino acids-mediated water oxidation pathway.

**Ozone Produced by Amino Acids Exhibits Bactericidal Activity in the Cell-Free System.** We next investigated whether an oxidant with the chemical signature of ozone produced by amino acids killed bacteria in our cell-free system. Bactericidal studies were performed on catalase-positive bacteria, *Escherichia coli*, NIHJ-JC2. In this experiment, to increase solubility in water, we used a variant of 6FP, 2-(*N*,*N*-dimethylaminomethyleneamino)-6-formyl-3-pivaloylpteridine-4-one (6FP-tBu-DMF), which generates singlet oxygen to a similar extent to 6FP (9). Viable *E. coli* were nearly undetectable with the addition of 6FP-tBu-DMF and amino acids (Trp or Met) after a 2-h irradiation, whereas 6FP-tBu-DMF alone had little effect on the viability of *E. coli* even with a 2-h irradiation (Fig. 3*A*). The administration of IgG together with 6FP-tBu-DMF exhibited a similar profile to these amino acids (data not shown). These results provide evidence to support the key role of these amino acids in bactericidal activity. The viability of *E. coli* was not affected by the addition of Arg or Phe, which had failed to exhibit catalytic activity for the generation of an oxidant with the chemical signature of ozone (Fig. 3*B*). Given that hydrogen peroxide ($H_2O_2$), which is highly bactericidal, is also the ultimate product of the water-oxidation pathway, it is rational to speculate that $H_2O_2$ might mediate the

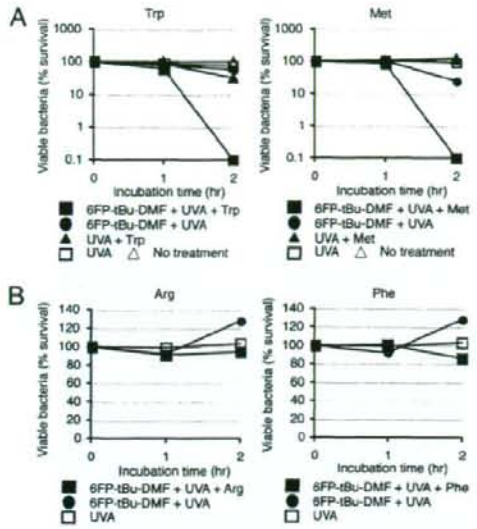


**Fig. 3.** Ozone produced by amino acids kills bacteria in the cell-free system. *E. coli* were incubated with or without 6FP-tBu-DMF and amino acids under UVA irradiation for 2 h. (*A*) Effect of Trp or Met on the survival of *E. coli*. The addition of both 6FP-tBu-DMF and amino acids exhibited strong bactericidal activity after a 2-h irradiation. (*B*) Effect of Arg or Phe on the survival of *E. coli*. Note that the amino acids showed no effects on bactericidal activity.

bactericidal activity observed. Quantification of $H_2O_2$ toxicity against *E. coli* revealed that $H_2O_2$ levels on treatment with 6FP-tBu-DMF and amino acids were ≈80 μM, which was completely repressed by catalase treatment (Fig. 4*A*). However, $H_2O_2$ levels required to kill 50% of the bacteria were ≈1–10 mM (Fig. 4*B*), suggesting that $H_2O_2$ is unlikely to be the principal contributor to the killing activity in this system.

**Ozone Production by Amino Acids in Human Neutrophils.** Next, we examined whether human neutrophils really have the functional capacity to produce ozone. We have identified a patient with a rare variant type of CGD carrying a defect in the gp91-*phox* component, whose granulocytes could produce significant amounts of singlet oxygen, but very little superoxide. Thus, neutrophils from this CGD patient should provide a useful model to allow the testing of our hypothesis in human neutrophils, because it is difficult to determine whether the amino

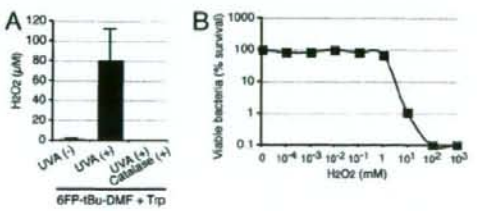


**Fig. 4.** $H_2O_2$ levels in the cell-free system. (*A*) $H_2O_2$ levels generated by 6FP-tBu-DMF and Trp after 2-h irradiation. Note that $H_2O_2$ production was completely repressed by catalase treatment. The data represent mean values ± SD ($n = 3$). (*B*) Concentration-dependent toxicity of $H_2O_2$ on the viability of *E. coli*. Increasing concentrations of $H_2O_2$ ($0–10^3$ mM) were added to the *E. coli*. The experiments were performed at least 3 times, and representative data are shown.

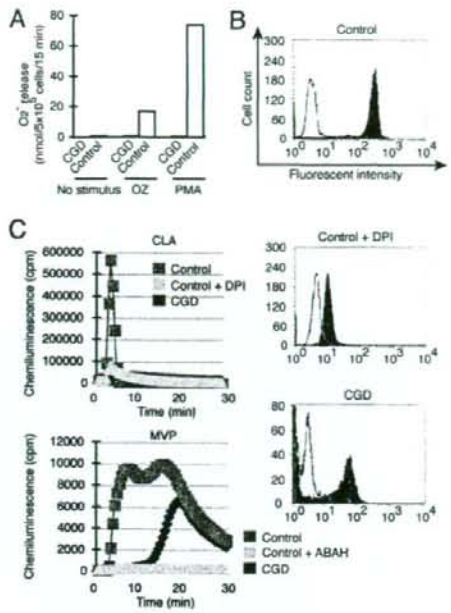


**Fig. 5.** Production of singlet oxygen with very little superoxide in a variant type of gp91-*phox*-deficient CGD neutrophils. (*A*) SOD-inhibitable reduction of ferricytochrome *c* in control and CGD neutrophils. Superoxide release was analyzed in unstimulated, OZ-stimulated, or PMA-stimulated neutrophils. (*B*) DHR assay in neutrophils from a healthy control (*Top* and *Middle*) and a CGD patient (*Bottom*). In *Middle* the pretreatment of control neutrophils with DPI, an inhibitor of NADPH-oxidase, is revealed. Fluorescence intensity is shown on the logarithmic *x* axis, and the cell count is shown on the *y* axis. (*C*) Superoxide (*Upper*) and singlet oxygen (*Lower*) release from control and CDG neutrophils. Neutrophils were incubated with CLA for superoxide detection or MVP for singlet oxygen detection, and luminescence was monitored every 30 s for 30 min. Some control neutrophils were pretreated with DPI for the CLA (*Upper*) or with ABAH, an inhibitor of MPO, for the MVA (*Lower*).

acid-catalyzed generation of ozone actually occurs in vivo by using healthy human neutrophils. Extracellular superoxide production was measured by the superoxide dismutase (SOD)-inhibitable reduction of ferricytochrome *c*. Neutrophils from a healthy control released substantial amounts of superoxide in response to stimulation with either phorbol myristate acetate (PMA) or opsonized zymosan (OZ). In sharp contrast, neutrophils from this CGD patient did not release detectable superoxide in response to either stimulus (Fig. 5*A*). We next used the fluorescent dye dihydrorhodamine (DHR) 123 in a flow cytometric assay to detect ROS. PMA-stimulated neutrophils from a healthy control revealed a significant increase in DHR fluorescence, which was counteracted by pretreatment with diphenyleneiodonium (DPI), an inhibitor of NADPH-oxidase (Fig. 5*B*). In contrast, neutrophils from the gp91-*phox*-mutated variant CGD patient exhibited a moderate fluorescence increase after PMA stimulation, reminiscent of the partial DHR response reported in p47-*phox*-deficient CGD patients (Fig. 5*B*) (11). To further verify the results, we used 2 chemiluminescent probes, 2-methyl-6-phenyl-3,7-dihydroimidazo[1,2-*a*]pyrazin-3-one (CLA) and *trans*-1-(2′-methoxyvinyl)pyrene (MVP), which were developed to specifically detect superoxide and singlet oxygen, respectively (10, 12–14). The pretreatment of control neutrophils with DPI abolished the CLA chemiluminescence, suggesting the specificity of this probe for superoxide detection (Fig. 5*C*). The

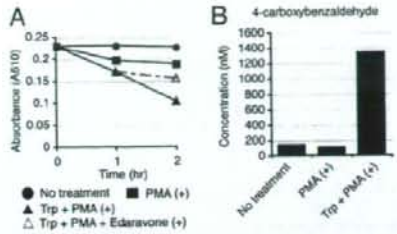


Fig. 6. Ozone production in a variant type of gp91-*phox*-deficient CGD neutrophils. (*A*) Effect of Trp on ozone production in activated CGD neutrophils. Indigo carmine was incubated with unstimulated or PMA-stimulated CGD neutrophils. Trp was added to PMA-stimulated CGD neutrophils to analyze ozone production. Loss of indigo carmine was monitored by measuring its absorbance at 610 nm. Note that a scavenger of singlet oxygen, edaravone, partially suppressed the reaction. The experiments were performed at least 3 times, and representative data are shown. (*B*) HPLC analysis of 4-carboxybenzaldehyde in CGD neutrophils. PMA-stimulated CGD neutrophils with Trp administration produced 4-carboxybenzaldehyde from vinylbenzoic acid.

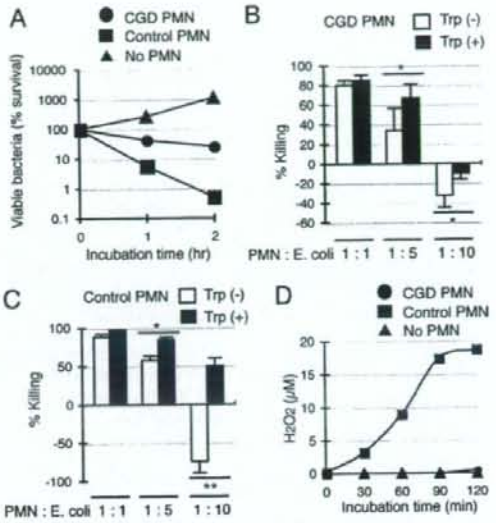


Fig. 7. Ozone produced by amino acids augments the bactericidal activity of neutrophils. (*A*) Bactericidal activity of CGD and healthy control neutrophils (PMN). *E. coli* were incubated with CGD or control neutrophils for 2 h. (*B* and *C*) Effect of Trp on the bactericidal activity of CGD (*B*) and healthy control (*C*) neutrophils. CGD or control neutrophils were challenged with increasing amounts of *E. coli* at a ratio of 1:1, 1:5, or 1:10 in the presence or absence of Trp. The data represent mean values ± SD ($n = 3$; *, $P < 0.05$; **, $P < 0.01$; paired *t* test). (*D*) $H_2O_2$ levels produced by CGD and healthy control neutrophils. The experiments were performed at least 3 times, and representative data are shown.

treatment of control neutrophils with 4-aminobenzoic acid hydrazide (ABAH), an inhibitor of myeloperoxidase (MPO), abrogated the MVP chemiluminescence (Fig. 5*C*). The CLA chemiluminescence in the variant CGD neutrophils was nearly undetectable, whereas the MVA chemiluminescence in the CGD neutrophils was approximately half of that in healthy control neutrophils, suggesting that the variant CGD neutrophils produced very small amounts of superoxide, but had the ability to produce singlet oxygen to some extent (Fig. 5*C*). To verify our results in the cell-free system, an oxidation reaction of indigo carmine was carried out on neutrophils from the variant CGD patient. Spectrophotometric assay revealed that the addition of Trp to PMA-stimulated neutrophils led to the successful conversion of indigo carmine to isatin sulfonic acids (Fig. 6*A*). A scavenger of singlet oxygen, edaravone, partially suppressed the reaction (Fig. 6*A*). HPLC analysis revealed that the PMA-stimulated CGD neutrophils with Trp administration produced 4-carboxybenzaldehyde from vinylbenzoic acid (Fig. 6*B*), substantiating the production of an oxidant with the chemical signature of ozone from singlet oxygen in human neutrophils.

**Ozone Produced by Amino Acids Augments Bactericidal Activity of Human Neutrophils.** Finally, we examined the bactericidal activity of neutrophils from the variant CGD patient. A bactericidal assay revealed that the CGD neutrophils were able to partially kill *E. coli* in a condition whereby the ratio of neutrophils to *E. coli* was 1:1, although the killing activity was less than that of healthy neutrophils (Fig. 7*A*). In the variant CGD neutrophils, the administration of amino acids, Trp and Met, augmented the bactericidal activity of neutrophils, which was more evident when the ratio of *E. coli* to neutrophils was high (>5:1) (Fig. 7*B* and data not shown). These results suggest that the formation of an oxidant with the chemical signature of ozone catalyzed by amino acids facilitate the bactericidal action of the variant CGD neutrophils. This beneficial effect of amino acids on bactericidal activity was also observed in healthy neutrophils, when higher doses of *E. coli* were added to neutrophils (Fig. 7*C* and data not shown). These results are indicative of a general role for amino acid-catalyzed ozone in the bactericidal action of human neutrophils. To examine the effect of $H_2O_2$ on the killing activity of neutrophils, we measured the $H_2O_2$ concentration by using a highly sensitive and stable $H_2O_2$ probe, *N*-acetyl-3,7,–2-phenylethylamine dihydroxyphenoxazine (15). In contrast to healthy neutrophils, the $H_2O_2$ level in the CGD neutrophils was negligible, indicating that $H_2O_2$ is unlikely to be relevant to the killing activity (Fig. 7*D*).

## Discussion

In this study, we showed that 4 amino acids, by themselves, were able to catalyze the production of an oxidant with the chemical signature of ozone from singlet oxygen in the water-oxidation pathway, comparably to antibodies. The resultant oxidant with the chemical signature of ozone exhibited significant bactericidal activity in our cell-free system and in human neutrophils. Ozone production by neutrophils is still a debatable issue. However, considering the findings of this study, where distinct model systems were exploited, we favor the proposal by Wentworth and colleagues (2–4) that antibodies can catalyze ozone generation in neutrophils. Our results further suggested the hypothesis that amino acids themselves exhibited catalytic activity to convert singlet oxygen and water to an oxidant with the chemical signature of ozone, and amino acid-catalyzed oxidant with the chemical signature of ozone showed bactericidal activity in human neutrophils.

What is the biological importance of ozone generated by neutrophils in host defense? MPO catalyzes the reaction to produce hypochlorous acid (HOCl) from hydrogen peroxide ($H_2O_2$) and chloride ion ($Cl^-$) (16). MPO deficiency is the most common congenital neutrophil defect. Despite the important role for HOCl in killing microorganisms, MPO-deficient individuals are usually healthy, in sharp contrast to CGD patients (17, 18). However, some MPO-deficient patients revealed an increased susceptibility to infections with bacteria and fungi, particularly those caused by *Candida albicans* (17, 19, 20). In agreement with these facts, MPO-deficient mutant mice, which failed to produce HOCl and subsequent singlet oxygen, showed

an increased susceptibility to pneumonia and death when challenged by high doses of bacteria and fungi, although they were generally healthy under normal conditions (21, 22). In human neutrophils we examined, the bactericidal activity induced by the addition of amino acids was prominent when larger numbers of *E. coli* were added to neutrophils (*E. coli*/neutrophils = 5:1 or 10:1), reminiscent of the MPO deficiency. Thus, ozone produced by neutrophils might potentiate a host defense system when the host is challenged by high doses of infectious agents.

Our current study further suggests the potential therapeutic role for amino acid-catalyzed oxidant with the chemical signature of ozone in infectious diseases. ROS have been playing a central role in photodynamic therapy (PDT) for cancer (23), where light and certain chemicals (photosensitizer) are used. The photosensitizer transfers energy from light to molecular oxygen to generate free radicals/radical ions or singlet oxygen. The ROS that are generated by PDT can kill tumor cells directly, damage the tumor-associated vasculature, and activate an immune response against tumor cells. PDT is now being applied to the treatment of many other diseases, including targeting of microorganisms (24). With an increase in antibiotic resistance, the development of new antimicrobial strategies is expected. In our distinct cell-free system, unexpectedly, the use of a potential photosensitizer, 6FP-tBu-DMF, and UVA, which produced singlet oxygen that is toxic, failed to kill bacteria (Fig. 3*A*). However, the addition of Trp or Met to 6FP-tBu-DMF and UVA, which produced an oxidant with the chemical signature of ozone, dramatically reduced the rate of viable bacteria (Fig. 3*A*). These results suggest that our study may contribute to the improvement of antimicrobial PDT.

## Materials and Methods

**Reagents.** Edaravone, human IgG, and human $F(ab')_2$ were kind gifts from Mitsubishi Pharma. 6FP was obtained from Sankyo Kasei Kogyo. 6FP-tBu-DMF was synthesized in our laboratories at the Institute of Advanced Energy, Kyoto University (9). CLA was purchased from Tokyo Kasei Kogyo; MVP, DHR, and the Amplex Red $H_2O_2$ kit were from Molecular Probes. Indigo carmine, gelatin, BSA, dextran, trisodium citrate dihydrate, acetonitrile, and sodium azide were from Nakalai; water-soluble amino acids were from Wako; heart infusion agar was from Nissui; Percoll was from GE Healthcare; zVAD-fmk was from the Peptide Institute; and $H_2{}^{18}O$ (> 97% $H_2O$) was from Cambridge Isotope Laboratories. Other chemicals, such as zymosan, FMLP, PMA, SOD, DPI, ABAH, catalase, tetrabutylammoniumhydrogen sulfate (TBA), isatin sulfonic acid, vinylbenzoic acid, and 4-carboxybenzaldehyde, were purchased from Sigma–Aldrich.

**Human CGD Patient.** The human CGD patient was a 25-year-old male with gp91-*phox* deficiency. Mutation analysis revealed a G-to-A point mutation at nucleotide 252 in exon 3, which produces an aberrant splicing site (25).

**Preparation of Neutrophils.** Human neutrophils were isolated from peripheral blood of healthy adult volunteers and the CGD patient by sedimentation through 2-step Percoll gradients, as described (26). Healthy volunteers and the patient provided written informed consent for participation in an institutional review board-approved protocol at Kyoto University Hospital.

**Ozone Production in the Cell-Free System.** A solution of indigo carmine (30 $\mu$M) and 6FP (40 $\mu$M) was irradiated for 4 min at 5 mW/cm$^2$ by using a UVA radiation apparatus (XX-15BLB 625 nm; UVP) in the presence or absence of human immunoglobulins [IgG and $F(ab')_2$] (5 mg/mL), BSA (5 mg/mL), FMLP (100 $\mu$M), zVAD-fmk (100 $\mu$M), or 19 water-soluble amino acids (1 mM) except for tyrosine. In this reaction, indigo carmine was converted to isatin sulfonic acids by ozone. Loss of indigo carmine was monitored by measuring its absorbance at 610 nm with a spectrometer (DU800; Beckman Coulter). For the dose–response reaction, increasing concentrations of Trp, Met, Cys, or His (1 $\mu$M to 2 mM) were added to the reaction in the presence of 6FP. Sodium azide (1 mM), edaravone (40 $\mu$M), and catalase (2,000 units/mL) were added to the reaction in the presence of 6FP to examine the effects on ozone production by IgG (5 mg/mL), Trp, Met, Cys, and His (1 mM). As a control, a sample without amino acids was analyzed. For HPLC analysis, indigo carmine (100 $\mu$M) or vinylbenzoic acid (30 $\mu$M) was mixed with 6FP (40 $\mu$M) and Met (1 mM) with or without UVA irradiation for 4 min. The samples were subjected to HPLC analysis.

**HPLC Analysis for the Detection of Isatin Sulfonic Acid and 4-Carboxybenzaldehyde.** The conversion of indigo carmine to isatin sulfonic acid and the oxidation of vinylbenzoic acid to 4-carboxybenzaldehyde were considered as evidence of ozone formation (6). Samples were analyzed on a reverse-phase $C_{18}$ HPLC column eluting with 70% 50 mM phosphate buffer (pH 7.2) containing 10 mM TBA and 30% acetonitrile with an L6000 Hitachi HPLC system (indigo carmine, $R_T$ = 12.0 min; isatin sulfonic acid, $R_T$ = 5.1 min; vinylbenzoic acid, $R_T$ = 15.3 min; 4-carboxybenzaldehyde, $R_T$ = 6.4 min) (3, 5). Peak areas were converted to concentrations by comparison to standard curves.

**Assay for Measuring $^{18}O$ Isotope Incorporation into Isatin Sulfonic Acid During Indigo Carmine Oxidation by Amino Acid-Catalyzed Water Oxidation.** An aliquot of indigo carmine (150 $\mu$M) in phosphate buffer (50 mM, pH 7.4) containing $H_2{}^{18}O$ (> 97% $H_2O$) was added to a solution of 6FP (40 $\mu$M) in the presence or absence of Met (600 $\mu$M) in phosphate buffer (50 mM, pH 7.4) containing $H_2{}^{18}O$ (>97% $H_2O$). The solution was irradiated for 4 min at 5 mW/cm$^2$ by using an UVA radiation apparatus. Production of isatin sulfonic acid was determined by LC to confirm that reaction had been successful before mass spectral analysis. LC conditions were a reverse-phase $C_{18}$ HPLC column and acetonitrile/water (10 mM ammonium acetate) (20:80) mobile phase at 1 mL/min (isatin sulfonic acid, $R_T$ = 2.1 min). MS was measured by using negative ion electrospray MS on a Waters Quattro micro API mass spectrometer. The raw data were extracted into Waters MassLynx version 4.0 format for presentation.

**Bactericidal Assay in the Cell-Free System.** *E. coli* NIHJ-JC2 ($5 \times 10^6$/mL) were incubated with or without 6FP-tBu-DMF (40 $\mu$M) and amino acids (Trp, Met, Arg, or Phe) (1 mM) under UVA irradiation (5 mW/cm$^2$) for 2 h. Samples were removed at 60 and 120 min and suspended in water. An aliquot of the suspension was plated on a pour plate made with heart infusion agar. After a 24-h incubation at 37 °C, the colonies formed were counted.

**$H_2O_2$ Production in the Cell-Free System and Human Neutrophils.** $H_2O_2$ production was measured by using a $H_2O_2$ probe, *N*-acetyl-3,7-dihydroxyphenoxazine (Amplex Red), including horseradish peroxidase (27). A solution of 6FP-tBu-DMF (40 $\mu$M) and Trp (1 mM), or PMA (50 ng/ml)-stimulated neutrophils ($5 \times 10^6$ cells), were incubated with 50 $\mu$M Amplex Red for 2 h at 37° C. Fluorescence was measured by a fluorometric microplate reader (Fluoroskan Ascent; Labsystems) with excitation and emission wavelengths of 544 and 590 nm, respectively. The amount of $H_2O_2$ production was calculated according to the standard curve of $H_2O_2$. To confirm the specificity of this assay, catalase (2,000 units/mL) was added to the reaction before incubation with Amplex Red.

**Bactericidal Effect of $H_2O_2$.** *E. coli* ($5 \times 10^6$/mL) was incubated with increasing concentrations of $H_2O_2$ ($0–10^3$ mM) for 2 h. Samples were removed at 2 h, and the bactericidal assay was performed as described above.

**Superoxide Release from Neutrophils.** Superoxide production was assessed by the SOD-inhibitable reduction of ferricytochrome *c* as described (28).

**Flow Cytometric DHR Assay.** Neutrophils ($5 \times 10^5$ cells) were loaded with 2 $\mu$M DHR for 5 min at 37 °C. After that, the cells were stimulated with 50 ng/ml PMA for 15 min at 37 °C and analyzed by flow cytometry. As a negative control, the pretreatment of neutrophils from a healthy control with 10 $\mu$M DPI, an inhibitor of NADPH oxidase, was performed before DHR loading.

**Chemiluminescence Assay.** The productions of superoxide and singlet oxygen of neutrophils stimulated with PMA were examined by using chemiluminescence with an $O_2^{\cdot-}$-specific probe, CLA, and an $^1O_2$-specific probe, MVP, respectively. After mixing the neutrophils ($2 \times 10^6$ cells) with 2.5 $\mu$M CLA or 40 $\mu$M MVP, the mixture was mounted on a luminescence reader (Aloka BLR-301), and the luminescence was monitored every 30 s for 30 min. As a negative control, the pretreatment of neutrophils from a healthy control with 10 $\mu$M DPI or 100 $\mu$M ABAH, an inhibitor of MPO, was performed.

**Ozone Production of CGD Neutrophils.** Indigo carmine (30 $\mu$M) was incubated with unstimulated or PMA (50 ng/mL)-stimulated CGD neutrophils ($1 \times 10^6$/mL) in the presence or absence of 1 mM Trp for 2 h at 37 °C. Edaravone (40 $\mu$M) was added to the reaction to examine the effect on ozone production. The loss of indigo carmine was monitored as described above. Vinylbenzoic acid (100 $\mu$M) was incubated with unstimulated or PMA (50 ng/mL)-stimulated CGD

neutrophils ($1 \times 10^6$/mL) in the presence or absence of 1 mM Trp for 2 h at 37 °C. The samples were subjected to HPLC analysis as described above.

**Bactericidal Assay of Human Neutrophils.** Bactericidal activity of human neutrophils was determined by a standard technique (29). Briefly, the reaction mixture contained $2.5 \times 10^6$ neutrophils, $2.5 \times 10^6$ (PMN:*E. coli* = 1:1), or $1.25 \times 10^7$ (1:5), or $2.5 \times 10^7$ (1:10) *E. coli* cells, 10% human AB serum, 0.1% gelatin, and HBSS. The mixture was incubated with or without 1 mM Trp at 37 °C. Samples were removed at 60 and 120 min, and the bactericidal assay was performed as described above.

**Statistical Analysis.** Data are expressed as the mean ± SD. $P < 0.05$ by the paired Student's *t* test was considered significant.

**ACKNOWLEDGMENTS.** We thank Dr. Hiroyuki Nunoi for genetic analysis of the CGD patient and Dr. Harry L Malech for helpful discussions. This work was supported by the Mitsubishi Pharma Foundation.

1. Williams R (2006) Killing controversy. *J Exp Med* 203:2404.
2. Wentworth P, Jr, *et al.* (2002) Evidence for antibody-catalyzed ozone formation in bacterial killing and inflammation. *Science* 298:2195–2199.
3. Babior BM, Takeuchi C, Ruedi J, Gutierrez A, Wentworth P, Jr (2003) Investigating antibody-catalyzed ozone generation by human neutrophils. *Proc Natl Acad Sci USA* 100:3031–3034.
4. Nieva J, Wentworth P, Jr (2004) The antibody-catalyzed water oxidation pathway: A new chemical arm to immune defense? *Trends Biochem Sci* 29:274–278.
5. Kettle AJ, Clark BM, Winterbourn CC (2004) Superoxide converts indigo carmine to isatin sulfonic acid: Implications for the hypothesis that neutrophils produce ozone. *J Biol Chem* 279:18521–18525.
6. Kettle AJ, Winterbourn CC (2005) Do neutrophils produce ozone? An appraisal of current evidence. *Biofactors* 24:41–45.
7. Malech HL (1993) Phagocyte oxidative mechanisms. *Curr Opin Hematol* 1:123–132.
8. Weening RS, Adriaansz LH, Weemaes CM, Lutter R, Roos D (1985) Clinical differences in chronic granulomatous disease in patients with cytochrome *b*-negative or cytochrome *b*-positive neutrophils. *J Pediatr* 107:102–104.
9. Yamada H, *et al.* (2005) Photodynamic effects of a novel pterin derivative on a pancreatic cancer cell line. *Biochem Biophys Res Commun* 333:763–767.
10. Sommani P, *et al.* (2007) Effects of edaravone on singlet oxygen released from activated human neutrophils. *J Pharmacol Sci* 103:117–120.
11. Vowells SJ, *et al.* (1996) Genotype-dependent variability in flow cytometric evaluation of reduced nicotinamide adenine dinucleotide phosphate oxidase function in patients with chronic granulomatous disease. *J Pediatr* 128:104–107.
12. Nakano M, Sugioka K, Ushijima Y, Goto T (1986) Chemiluminescence probe with cypridina luciferin analog, 2-methyl-6-phenyl-3,7-dihydroimidazo[1,2-a]pyrazin-3-one, for estimating the ability of human granulocytes to generate $O_2^-$. *Anal Biochem* 159:363–369.
13. Posner GH, *et al.* (1984) A chemiluminescent probe specific for singlet oxygen. *Biochem Biophys Res Commun* 123:869–873.
14. Teixeira MM, Cunha FQ, Noronha-Dutra A, Hothersall J (1999) Production of singlet oxygen by eosinophils activated in vitro by C5a and leukotriene B4. *FEBS Lett* 453:265–268.
15. Yamashita K, *et al.* (2001) 6-Formylpterin intracellularly generates hydrogen peroxide and restores the impaired bactericidal activity of human neutrophils. *Biochem Biophys Res Commun* 289:85–90.
16. Klebanoff SJ (2005) Myeloperoxidase: Friend and foe. *J Leukocyte Biol* 77:598–625.
17. Parry MF, *et al.* (1981) Myeloperoxidase deficiency: Prevalence and clinical significance. *Ann Intern Med* 95:293–301.
18. Suzuki K, Muso E, Nauseef WM (2004) Contribution of peroxidases in host-defense, diseases, and cellular functions. *Jpn J Infect Dis* 57:51–52.
19. Lehrer RI, Cline MJ (1969) Leukocyte myeloperoxidase deficiency and disseminated candidiasis: The role of myeloperoxidase in resistance to *Candida* infection. *J Clin Invest* 48:1478–1488.
20. Nguyen C, Katner HP (1997) Myeloperoxidase deficiency manifesting as pustular candida dermatitis. *Clin Infect Dis* 24:258–260.
21. Aratani Y, *et al.* (1999) Severe impairment in early host defense against *Candida albicans* in mice deficient in myeloperoxidase. *Infect Immun* 67:1828–1836.
22. Aratani Y, *et al.* (2000) Differential host susceptibility to pulmonary infections with bacteria and fungi in mice deficient in myeloperoxidase. *J Infect Dis* 182:1276–1279.
23. Dolmans DE, Fukumura D, Jain RK (2003) Photodynamic therapy for cancer. *Nat Rev Cancer* 3:380–387.
24. Maisch T (2007) Antimicrobial photodynamic therapy: Useful in the future? *Lasers Med Sci* 22:83–91.
25. Roos D, *et al.* (1996) Mutations in the X-linked and autosomal recessive forms of chronic granulomatous disease. *Blood* 87:1663–1681.
26. Moriguchi T, *et al.* (1990) Studies of the functions of polymorphonuclear leukocytes obtained from human bone marrow. *Acta Hematol Jpn* 53:668–677.
27. Zhou M, Panchuk-Voloshina N (1997) A 1-step fluorometric method for the continuous measurement of monoamine oxidase activity. *Anal Biochem* 253:169–174.
28. Asagoe K, *et al.* (1998) Down-regulation of CXCR2 expression on human polymorphonuclear leukocytes by TNF-α. *J Immunol* 160:4518–4525.
29. Johnston RB, Jr, *et al.* (1975) The role of superoxide anion generation in phagocytic bactericidal activity. Studies with normal and chronic granulomatous disease leukocytes. *J Clin Invest* 55:1357–1372.

THE JOURNAL OF BIOLOGICAL CHEMISTRY VOL. 283, NO. 36, pp. 24420–24425, September 5, 2008


# Acetylation of PML Is Involved in Histone Deacetylase Inhibitor-mediated Apoptosis*[S]

Received for publication, March 20, 2008, and in revised form, July 7, 2008 Published, JBC Papers in Press, July 11, 2008, DOI 10.1074/jbc.M802217200

**Fumihiko Hayakawa**[‡1], **Akihiro Abe**[‡], **Issay Kitabayashi**[§], **Pier Paolo Pandolfi**[¶], **and Tomoki Naoe**[‡]

*From the* [‡]*Department of Hematology and Oncology, Nagoya University, Graduate School of Medicine, Nagoya 466-8550, Japan, the* [§]*Molecular Oncology Division, National Cancer Center Research Institute, 5-1-1 Tsukiji, Chuo-ku, Tokyo 104-0045, Japan, and the* [¶]*Cancer Genetics Program, Beth Israel Deaconess Cancer Center, Department of Medicine, Harvard Medical School, Boston, Massachusetts 02215*

**PML is a potent tumor suppressor and proapoptotic factor and is functionally regulated by post-translational modifications such as phosphorylation, sumoylation, and ubiquitination. Histone deacetylase (HDAC) inhibitors are a promising class of targeted anticancer agents and induce apoptosis in cancer cells by largely unknown mechanisms. We report here a novel post-transcriptional modification, acetylation, of PML. PML exists as an acetylated protein in HeLa cells, and its acetylation is enhanced by coexpression of p300 or treatment with a HDAC inhibitor, trichostatin A. Increased PML acetylation is associated with increased sumoylation of PML *in vitro* and *in vivo*. PML is involved in trichostatin A-induced apoptosis and PML with an acetylation-defective mutation shows an inability to mediate apoptosis, suggesting the importance of PML acetylation. Our work provides new insights into PML regulation by post-translational modification and new information about the therapeutic mechanism of HDAC inhibitors.**

The promyelocytic leukemia protein PML controls cell cycle progression, senescence, and cell death (1, 2). Wild-type PML is a potent growth suppressor that, when overexpressed, can block cell cycle progression in a variety of tumor cell lines (1); conversely $PML^{-/-}$ mouse embryo fibroblasts (MEFs)[2] replicate significantly faster than their $PML^{+/+}$ MEFs (3). PML also plays an essential role in DNA damage or stress-induced apoptosis, and $PML^{-/-}$ cells are resistant to a variety of apoptotic signals (4). In normal cells, the PML protein is localized in, and essential for the biogenesis of, discrete subnuclear compartments designated as nuclear bodies (NBs) (5). In NBs, PML coaccumulates with more than 70 kinds of proteins that are involved in tumor suppression, apoptosis, regulation of gene expression, anti-viral response, and DNA repair. PML is thought to exert its function by regulating the function of binding partners as a core of NBs (6). Intriguingly, NBs are disrupted in human acute promyelocytic leukemia cells by PML-RAR$\alpha$, a oncogenic fusion protein of PML, and RAR-$\alpha$, which is thought to be the mechanism of anti-apoptotic effect of PML-RAR$\alpha$ (7–9).

It has been reported that NB formation requires PML to be conjugated to SUMO-1 (5, 10). SUMO-1 is an 11-kDa protein that is structurally homologous to ubiquitin (11). Sumoylation is thought to regulate the subcellular localization, stability, DNA binding, and/or transcriptional ability of its target proteins such as PML, Ran GTPase-activating protein (RanGAP)1, I$\kappa$B$\alpha$, and heat shock transcription factor 2 (11). Virtually $As_2O_3$, a chemotherapeutic agent clinically used in the treatment of acute promyelocytic leukemia cells, induces PML sumoylation. Increased PML sumoylation induced by $As_2O_3$ treatment leads to the restoration of NBs disrupted by PML-RAR$\alpha$ and then is followed by apoptosis in acute promyelocytic leukemia cells, which results in prolonged remission of the disease (12–15). These findings underscore the importance of PML sumoylation and the integrity of NBs to tumor suppression.

Histone deacetylase (HDAC) inhibitors, a promising class of targeted anticancer agents, can block proliferation and induce cell death in a wide variety of transformed cells (16). HDAC inhibitors block the activity of class I and II HDACs and induce histone acetylation, which leads to the relaxation of chromatin structure, enhanced accessibility of transcription machinery to DNA, and increased gene transcription (17). HDAC inhibitors also induce acetylation of transcription factors, which alters their activities and the expression of their target genes (18). Recent studies demonstrated that p53 acetylation induced by a HDAC inhibitor leads to expression of proapoptotic proteins such as Bax, PIG3, and NOXA (19, 20). However, the mechanisms of p53-independent apoptosis by HDAC inhibitor remain largely unknown.

Here, we report PML acetylation as its novel post-transcriptional modification. PML acetylation is induced by trichostatin A (TSA), a HDAC inhibitor. This enhanced acetylation leads to increased PML sumoylation and may play a key role in TSA-induced apoptosis. This work provides new insights into the

* This work was supported by grants-in-aid from the Uehara Memorial Foundation, the National Institute of Biomedical Innovation, and the Ministry of Education, Culture, Sports, Science, and Technology of Japan. The costs of publication of this article were defrayed in part by the payment of page charges. This article must therefore be hereby marked "*advertisement*" in accordance with 18 U.S.C. Section 1734 solely to indicate this fact.

[S] The on-line version of this article (available at http://www.jbc.org) contains supplemental Fig. S1–S9 and supplemental data.

[1] To whom correspondence should be addressed: Dept. of Hematology and Oncology, Nagoya University, Graduate School of Medicine, 65 Tsurumai-cho, Showa-ku, Nagoya, 466-8550, Japan. Fax: 81-52-744-2161; E-mail: bun-hy@med.nagoya-u.ac.jp.

[2] The abbreviations used are: MEF, mouse embryo fibroblast; HDAC, histone deacetylase; TSA, trichostatin A; NB, nuclear body; RAR, retinoic acid receptor; SUMO, small ubiquitin-like modifier; HAT, histone acetyltransferase; GST, glutathione *S*-transferase; HA, hemagglutinin; GFP, green fluorescent protein.